Universidad de La Laguna

LA LAGUNA UNIVERSITY

SCIENCE FACULTY

MASTER DEGREE IN RENEWABLE ENERGIES

2021

“Implementation of a liquid air storage system (LAES) in a mixed renewable energy system (wind and photovoltaic). The case of Tenerife.”

Author:
Juan Felipe Castellanos Salazar

Supervisors:
Dr. Francisco Javier Ramos Real
Asst. Prof. Alfredo Jesús Ramírez Díaz

CONTENTS

INDEX OF FIGURES

INDEX OF TABLES

1. INTRODUCTION

In the European islands, the energy transition to renewable has been carried out in the same way as in continental territories, reaching in some islands to the European objectives [1]. The Canary Islands has a registered share of renewables of 16 % in electric generation near to the European policy and strategy in 2020 [2]. In these territories the renewable sources have difficulties that prevent the rise of its introduction in the electricity grid, due to the uncertainty of availability of the wind resource. The small sizes of the different isolated electrical systems in Canaries make the integration of renewables more difficult, due the criteria about the security of the electric supply given by Transmission System Operator (TSO). One way to overcome these limitations is interconnecting the islands, increasing the resilience of the electrical grids. However, the depth of the sea and the cost are insurmountable barriers to implement this solution in La Palma and El Hierro, which will remain isolated [3].

The transition to renewable energies must be directed with technologies that overcome these technical difficulties and exploit all the potential installed, where storage systems are one of the other solutions [4],[5]. The energy storages could save the surplus from renewable energy and inject into the system later. For example, some studies have concluded that the thermal and electrochemical energy storage systems connected into the grid could give higher revenues and a reduction of almost 15% of CO2 emissions [6].

Focusing on the storage systems, these can be catalogued according to its principle of operation, such as mechanical with flywheels, thermal as compressed air (CAES) and Pumped Hydro Storage (PHS); electrochemical as lead acid and lithium batteries; chemical such as hydrogen among other. Each type has demonstrated technical and economic advantages according to its application in the electrical network [7]. Lithium batteries are according to the literature, the best alternative to storage energy and the most technologically advanced in many applications for the electrical services, giving the lowest investment cost [8].

In thermal energy storage, the Liquid Air Energy Storage (LAES) is the technology that in the last years has generated interest [9]. The advantages compared to other available technologies are: (i) longer life cycle than lithium batteries and (ii) occupies less space than PHS [10],[11]. The experience of this technology has been translated from the refrigeration industry[1], where using cleaned air how principal resource, this is compressed and cooled to its liquefaction temperature (-196 °C); after, the liquified air is stored in a cryogenic tank, where the air composition is mostly liquid nitrogen (with the possibility to obtain also liquified oxygen), this being the process of charge of the system. On the discharge stage, the liquid air is pumped and expanded until the air flow reaches its gaseous state again moving a special turbine that generates electricity [12].

As main advantages of LAES, this can be integrated with other conventional generations systems, for example, in the combustion of gas turbines, that using the oxygen obtained from the liquefaction in the process of charge to improve the efficiency of combustion of the natural gas and reducing the pollutant gases generated [13]. However, the air liquid storage is a system still under development field, where there is only one real pilot plant working in 2020, located in Slough, UK, which provides support in the network of this

[1] https://www.airliquide.com/industry/industrial-cryogenics: Applications and products of Industrial cryogenic and Liquid Air. Visited on 02-01-2021.

municipality, which has achieved RTE[2] being around 8%, lower than other storage technologies and being less minor than the maximum theoretical obtained of 70% [10], [12].

Seasonal availability is not the only limitation that LAES can overcome how storage systems, the space limitation and location are advantages to apply in islands. This system overcomes these problems because it has a theoretically higher energy densities, meaning within the same land space as CAES and PHS technologies, it can store a greater amount of energy [14]. Tenerife have a lack of availability of the land, given that 48.6% of the insular territory is protected, where LAES it turns out to be an opportunity to develop new storage technologies of reduced size and longer operating time for its application in the current electricity network [15]. By increasing the amount of clean energy that can be fed into the grid, these systems could additionally achieve a more sustainable system in the future, helping to reduce energy poverty [16].

The studies of application of LAES technology have focused recently on increasing the RTE and at the same time, in reducing the cost of the energy storage and injection in the electrical grid. The air liquid system combined with conventional and renewable generation systems, how Liquified Natural Gas (LNG) process, has been reached giving a cost of energy injected to the grid of LCOE[3] between 142 $/MWh and 205,0 $/MWh, closed with generation technologies like gas or nuclear [13],[17]. Comparing with storage systems, the levelized cost of the energy stored LCOS[4] in some studies have reached values of 150 €/MWh, close to technologies such as lithium batteries [7].

The aim of this research is to find the technical and economic viability in Tenerife of the application of LAES systems integrated with renewable energies, taking a mixed wind and photovoltaic generation plants as a case study of this integration for the island. The technical analysis will carry out structuring a state of the art of this technology, obtaining from literature the parameters for the modelling and developing a LAES plant. The economic assessment will provide the information about the investment, the LCOE among others economic metrics which will detail the feasibility of integrating these systems with renewable energies into Tenerife electricity network in the future, in turn, generating a new knowledge base for the implementation in these technologies in islands.

According to above, the project is divided by follows:

In section 2 will show a description of the electrical network in Tenerife, defining the characteristics of this system, to know the singularities of the system which the project must address. In section 3 a methodology will be designed, proposing that will summarize the process of creation of the scenarios, defining and develop two possible scenarios in Tenerife, where each one would have the year 2025, 2030 and 2035 to show the prospected growth of renewables. Also, a theoretical study plant conformed with renewables energies is defined, that would be working in each scenario and to which the LAES system would be integrated. In section 4 a methodology of design the different sizes of LAES adequate for the study plant is developed. Section 5 will detail the

[2] Round-Trip Efficiency RTE is the energy available in discharge above the energy consumed in charge.

[3] LCOE is the levelized cost of energy, calculated with the sum of the average cost of generating electricity over the energy produced in the time that the system will work.

[4] LCOS is the levelized cost of storage, calculated with the sum of the average of the cost of storage energy (the energy to the storage system is not paid for) in a system over the energy stored in the time that the system stores energy.

technical results obtained in terms of energy of the Liquid Air technology integrated with the study plant. The techno-economic analysis will be detailed in section 6 and finally, section 7 will explain the conclusions obtained from the project, processes of improvement and prospects for LAES and storage systems on the island.

2. POWER GENERATION SYSTEM AND DISPATCH IN TENERIFE

The electrical system of the island of Tenerife will be detailed in this chapter, focusing on the technical singularities, technologies in the generation systems and the market regulation that applies in the sector of the electrical network of Canary Islands. These information are important in order to know the parameters that could affect the construction of simulation of the future scenarios. According to the Canary Islands Energy Yearbook (2019), Tenerife has the largest installed power capacity with 1,426 MW, (around 43% of the total in Canaries) (see *Figure 1)* [1].

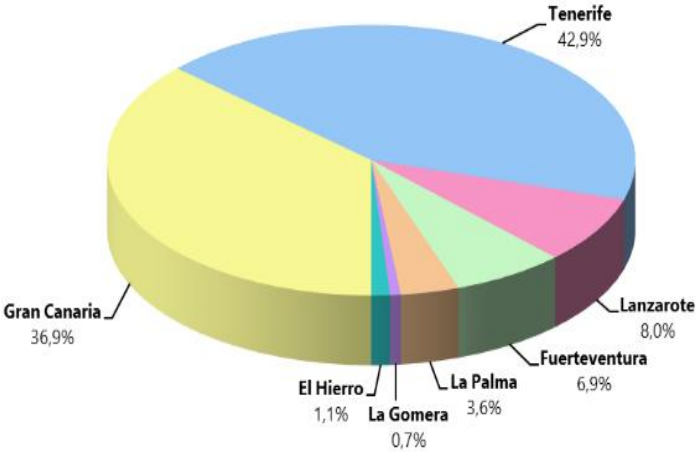

Figure 1. Percentage distribution of electrical power divided by Island. Source [2].

On the one hand, Decomposing the installed power, in *Table 1* is shown that in Tenerife has multiple conventional plants of thermal power that could provide 1,046 MW. The thermal power plants are composed of technologies such as combined cycle, gas turbines, steam plants and diesel engines. In other hand, the installed power of renewables energies in Tenerife comprises 197 MW of wind onshore, 116 MW of solar photovoltaic, 2.8 MW of mini-hydraulic and biogas systems, resulting in a total of 314.5 MW of renewable installed power.

Table 1. Generation Park Tenerife in 2019.

Technology	Power [MW]
Thermal Power	*1046.5*
Refinery	*25.9*
Cogeneration	*39.2*
Conventional	***1111.6***
Wind	*195.65*
Photovoltaic	*116.07*
Mini-hydraulic	*1.2*
Biogas	*1.6*
Renewable	***314.53***
TOTAL	***1426.13***

Figure 2 shows that a 78 % of the potential comes from conventional groups that used fossil fuel where the other 22 % corresponded to renewable energies, with a majority participation of wind energy over photovoltaic. Decomposing the graph, in 2019 the wind power was renewable with a major power installed with a 13.7% of general participation in the generation.

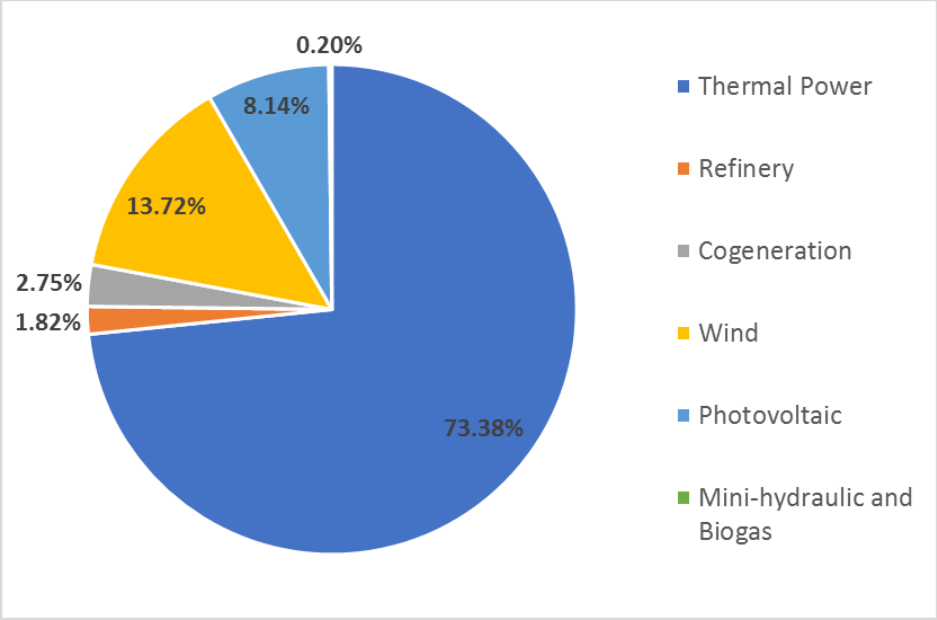

Figure 2. Electrical Power in Tenerife. Source: Anuario Energético de Canarias 2019 [2].

The increase of renewable energy power installed is not the only way to increase the consumption of this moving conventional energy. Technologies like massive storage systems or interconnection with other electrical systems in some cases add a support for renewable sharing in the grid, where compared with other islands in Canary, Tenerife does not have these technologies. For example, El Hierro has a unique system of PHS fed by wind energy, resulting in several days without conventional energy production [18]. Some studies have been carried out for its implementation of a similar system in other Canary islands such as La Palma and Gran Canaria obtaining promising results [3].

Alternative to storage systems, the interconnection of insular power grids supports the variability of the renewables, where Lanzarote - Fuerteventura connection is unique in the archipelago. Besides, a recent techno-economical study has concluded that developing an interconnection in Tenerife - La Gomera could provide a solution to electrical problems in this island in the long term [19].

In spite of the singularities of the Canary Islands, in general these islands are configured technically with a similar electrical network hierarchy that the peninsular networks, where the energy transmission networks are supervised by a TSO (Red Eléctrica de España) [20]. The electricity market involving the exchange of energy in this network is carried out by OMIE (Operador del Mercado Ibérico de Energía) [21]. However, due to the insular status, the electricity market and the injection of energy is managed differently from the peninsula system, where the economical dispatch is defined how the primary dispatch of electrical energy, establishing different parameters to the generators to inject energy according to the source of the energy regulated by the RD 738/2015 [22].

The renewable energies in the island have an advantage to reduce its cost in the energy market, because its variable costs of fuel and emission costs are zero, increasing the possibility to inject first energy because it has a lower cost than conventional. A recent study concludes that the cost parity in renewable, both solar and wind has been achieved in Canary Islands [23]. However, the stochastic production of renewables has made it difficult to inject energy constantly and plenty in the grid, due the possibility to destabilize the system when renewable energy drastically declines, generating a possible blackout. For this reason, interconnections and storage systems have been proposed and applied in the Canary Islands, in order to increase the share of renewable energy and maintain a balance in power flow.

At present, the energy storage technologies have not a special framework and market regulation, thus it uses the same regulation as renewables or a specific one for each plant (case of Gorona del Viento) [24]. Therefore, the storage systems have an economic disadvantage to inject energy in the grid compared with renewable and conventional systems, where this has concerned investors in renewable energy with storage to set up projects due the lack of polities in this theme.

3. METHODOLOGY

With the objective to create adequate scenarios in the project, the parameters of conventional and renewable energy power in Tenerife for the application of storage systems were defined first. This chapter will detail the methodology used for the creation and simulation of these scenarios, considering the characteristics of the generation system in the electrical network, and establishing an evolution of installed electrical potential on Tenerife. Compiling databases from REE and renewable growth targets set by government entities, the percentage growth of renewable energies was built, allowing to maintain the balance and equilibrium of the network with conventional systems.

In *Figure 3* is detailed the methodology applied for the development of the project: first were defined two scenarios based on data founded and related with the growth of renewables in Canary Islands, how polities, reports and renewables projects are in process to build in Tenerife [2],[25],[26],[27]. Defined each scenario, three representative years to future was selected to show the evolution of the growth of renewables, additionally, a theoretical battery without specified technology is applied in the electrical grid in each scenario, to support the renewables energies in the evolution of the generation. Parallel, the renewable study plant described before was introduced in each scenario, obtaining the renewable energy injected and surpluses by this plant.

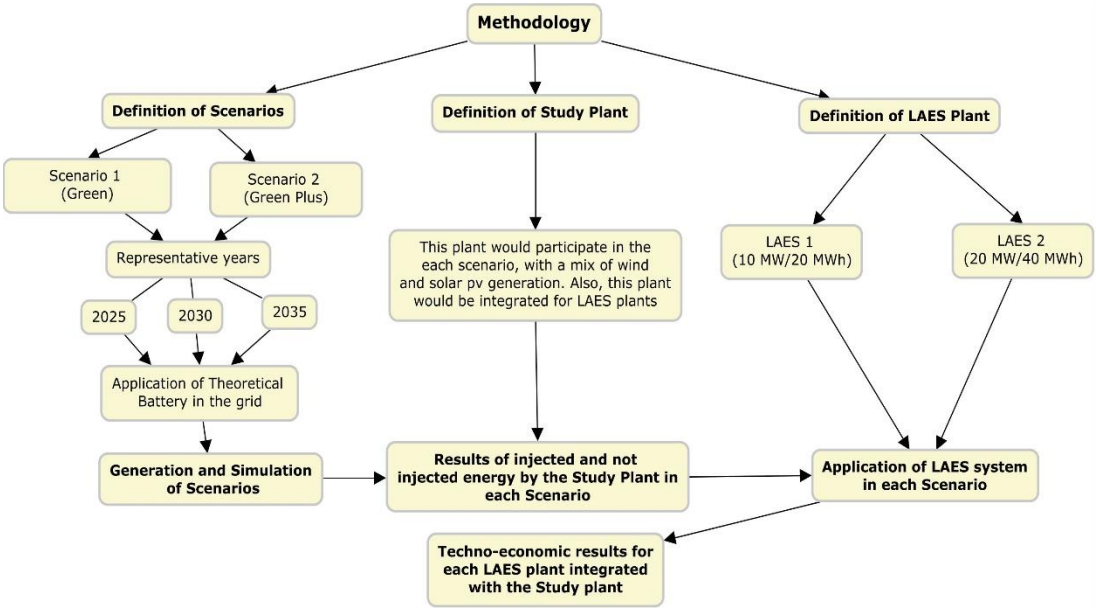

Figure 3. Schematic process of the methodology used in the project.

The renewable system object of the study case, specifically, a study plant that will apply the LAES is defined in this chapter, where it will consist of wind and photovoltaic energy that will be installed and participate in the generation system of the grid in each simulated scenario. The above with the objective of knowing the excess energy that this study plant could generate in each scenario and know of that energy which is usable to store in the LAES plant.

As it is expected that in the evolution of renewable energy in the scenarios, the energy not injected by the study plant will grow. In this case, the two LAES plants with different sizes were proposed, analyzing two different dispatches orders modes: (i) inject energy immediately when there is not renewable surplus (quick response); (ii) if the batteries had the capacity to store part of the energy not injected and saving this energy as a reserve to the grid (reserve response).

Finally, in accordance with the previous technical part, the economic study is evaluated. Using the investment cost, discount rate, lifetime and energy injected in each scenario, the LCOE is calculated. The economic analysis is based on NPV, IRR and Payback concepts. Furthermore, a sensitive study was carried out varying the price of the energy sold by the LAES.

3.1. Definition of the scenarios in Tenerife

Two different scenarios are proposed varying in terms of renewable installed capacity along the years of 2025, 2030 and 2035. The first scenario (called *Green Scenario)* is based on the current renewable capacity in construction and processed with the regional government. The second scenario (called *Green Plus Scenario)* is designed with higher growth compared to the first scenario. The Green Plus is aligned with the objective set out in PNIEC (Plan Nacional Integrado de Energía y Clima) based on the Europe 2030 energy objectives (nearly 70% of renewable share in electricity systems). For each scenario, the criteria of security of the operations have been considered using variables such as minimum conventional operation, conventional capacity installed and other massive energy storages in the islands (installation of batteries). These considerations have been proposed to cope with the maximum penetration of renewables as possible, but always under the requirements of security of the system.

3.1.1. Definition of the baseline year (2019)

For the development of the simulation model, the data from the electrical system of Tenerife in 2019 was taken. This year was representative in the reference to renewable resource, electrical demand and energy production (In contrast to 2020 that was the year altered with COVID-19). Some system operation data more interesting for 2019 is shown in *Table 2.* Likewise, during the days of higher renewable penetration, it was possible to establish the technical minimum of the operation of the system (80 MW of combined cycle and 45 MW of gas turbine) [25].

Table 2. Summary of the renewable electrical generation in Tenerife, 2019.

Parameter	Unit	Value
Max value share of Wind	MW	181,90
Max value share of PV	MW	99,80
Wind Onshore Power Installed	MW	195,64
Photovoltaic Power Installed (Including Self consumption)	MW	118,65
Max value share of Renewables	%	62,98
Renewable energy generated in 2019	GWh	686,37
Electrical generation in 2019	GWh	3576,82
Share of wind in the generation	%	13,88
Share of PV in the generation	%	5,31
Share of Renewables in the generation	%	19,19

In addition to the previous data, 2019 is taken as the basis for the hourly wind and solar resource profiles for the island of Tenerife. This will allow this project to use a simulation model to see what wind or solar production would be like with a higher installed capacity for future representative year on scenarios (2025, 2030 and 2035).

The base data of 2019 was obtained from the information of the demand viewer of the REE [25]. This represents the injected electricity generation in Tenerife for each type of technology and the demand, where these data are in 10-minute format per data, resampling the data per hour to facilitate the processing of the data in the build of the scenarios. The data obtained was cleaned up and processed, where the biogas and mini-hydraulic technologies are excluded due to its low participation in generation. The year 2019 was selected due to the growth of renewables in Tenerife this year, representing recent data for the elaboration of the simulation.

With the processing of the information of generation systems based on the year 2019, the following representation of *Figure 4* was obtained, detailing each system's participation in electricity generation connected in network for this year; for conventional energies, the combined cycle energy was the majority participation in generation throughout the year, followed by Steam turbine, diesel motor and gas turbine. With the renewable's energies, it is detailed that in this year wind power production surpassed photovoltaic production.

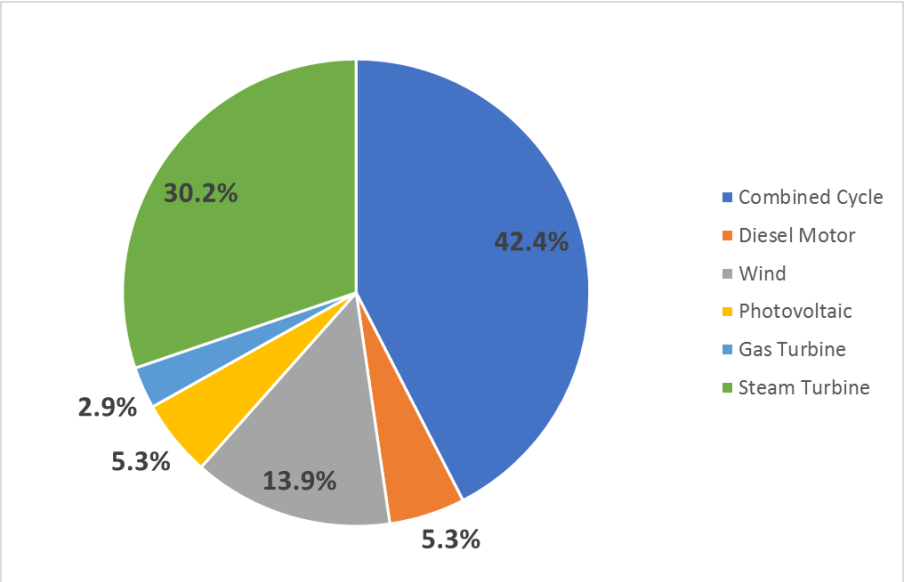

Figure 4. Participation of each generation system electrical grid in Tenerife in 2019.

3.1.2. Growth of Conventional Energies and Electrical Demand in the Future Scenarios

In the construction of the scenarios with the before information, the conventional energies must be participating with defined parameters to have a stability against the growth of renewable energy in the system. For this study, it is proposed that conventional should cover at least 30% of the electrical demand, that is, the maximum injection of the renewable energy hour by hour will be limited to 70% of the coverage of the demand.

Focusing on the conventional energies and due the combined cycle is the technology with the minor cost of electricity generation also being a “must run” unit (must be in operation), this system will provide the energy in the cases where the renewable energy does not cover 70%, acting as an energy primary regulator. When the combined cycle was not enough, the second regulator the steam turbine was defined, followed by the gas turbine and finally the diesel engine showed third and four regulators, respectively.

To complement a better introduction of renewable energies, it was proposed that the steam turbines must be decommissioned in the future, where this proposal was applied in all scenarios starting from the year 2030. From this year, the gas turbine is the second regulator and third the diesel engine. With above, the renewables must create an opportunity to inject more energy in the grid, trying to cover the participation in grid left by steam turbines,

Finally, electrical demand plays an important factor in the evolution of these scenarios, therefore for this project it was proposed that demand would grow by around 1.2% between years. This has been assumed to follow the growth of renewable energy and to prevent new demand that may be created in the energy transition process to 2030, e.g. electric vehicles [28],[29].

3.1.3. Detailed Growth of Renewable Energies in the Scenarios

The first scenario *Green* was defined with a growth of the renewable power in Tenerife, taking as a base the processed power of wind and solar to be installed in the island by 2019 and prospecting that by 2029, all this processed potential of wind and a plus of double of photovoltaic power will be installed and working in the network. The data of

processed potential was obtained from GrafCan Viewer, relating each park processed when was possible, with the state bulletins and official bulletins of Canary Islands (BOC), to verify the veracity of the data. The renewable power installed to work for 2019 was obtained from the Energy Yearbook. With the previous information, the growth of photovoltaic and wind power for any year between 2019 and 2029 was obtained, managing to apply this growth for the selected years like 2030.

The second scenario *Green Plus* was built was taken as a basis the PNIEC (Plan Nacional Integrado de Energía y Clima), being the target year 2030. In this national plan, the objectives are that 74% of the total electricity generation should come from renewable energies, around 42% of the total energy consumption should be covered by these energies and the energy efficiency should be 39,5%. This plan is based on the *Framework on Climate and Energy* for 2030, where the objective of the electricity generation of the 74% renewable in electrical demand was considered to create this scenario.

Due to the proposed limitation of 70% of renewable energies to the grid in the construction of the scenarios, it would make it difficult to obtain the objective of 74% proposed in *Green Plus Scenario*, for this reason a percentage decrease was made in renewables energies. Compared to the *Green* with *Green Plus Scenario*, in *Table 3* shows that in year-on-year growth of around 3-4% more. The reason that in the growth that would cover PNIEC target of 74% renewable, a higher growth of these power would be necessary, could generate an excess of non-injected energy and opportunity of storage of more energy. The complete development of the scenarios is in Appendix 1.

Table 3. Wind and PV growth prospect in [%] for Green and Green Plus Scenarios.

Renewable Technology	Green Scenario	Green Plus Scenario
Wind	8.65	10.77
Photovoltaic	6.52	10.98

A background for the development of storage technologies with renewable systems was taking into account the regulation RD-Law 23 of 2020 in Spain, that promotes the introduction of renewables with storage in the electrical system [30]. Therefore, to promote storage systems in the scenarios, the installation of a battery connected to the grid was considered, starting in 2025 with a power of 50 MW and 100 MWh of energy storage, increasing in the year 2030 and 2035 the double of power and energy storage (100 MW of power and 200 MWh of energy storage). The previous storage system will approach the 80% of the stored energy to be injected into the grid (*RTE = 0.8*). The *Table 4* summary the scenarios considered and developed to the implementation of the LAES system with the study plant.

Table 4. Summary of proposed scenarios.

Scenarios	Detail	Year of study	Storage system for each scenario
(1) Green	Installed and processed power from renewable energy (Dic-2019)	2025	50MW/100MWh from 2025
		2030	100MW/200MWh from 2030
(2) Green Plus	Base in PNIEC, close to 74% of share of renewables in electrical demand	2035	100MW/200MWh from 2030

With the definition of the scenarios, the *Figure 5* shows the increase of power installed in the *Green Scenario,* where the renewable energies power in 2035 almost 3 times of the base year 2020. It should be noted that in this scenario, the growth of wind power is notable compared to photovoltaic, the above because the data of processed renewable energy found, shows that in Tenerife most of the projects were wind onshore power.

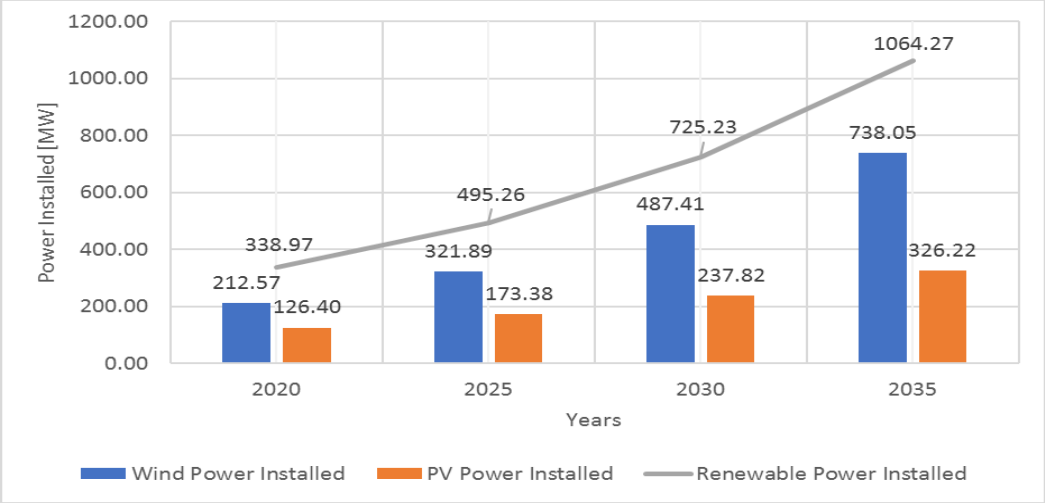

Figure 5. Power Growth of Renewables Energies [MW] in Scenario 1 – Green.

The *Figure 6* represents the *Green Plus*, which in comparison to *Green Scenario* has a steeper line in the renewable potential. This is due the growth of both wind and photovoltaic are higher than in the previous scenario, for example, the installed potential in 2035 that is four times higher than in 2020. The comparison with the *Green Scenario* is not only on the general renewable potential, the wind and photovoltaic have a smaller power difference in the evolution of the scenario, thus generating a more equal participation in the energy generation to cover the electrical demand.

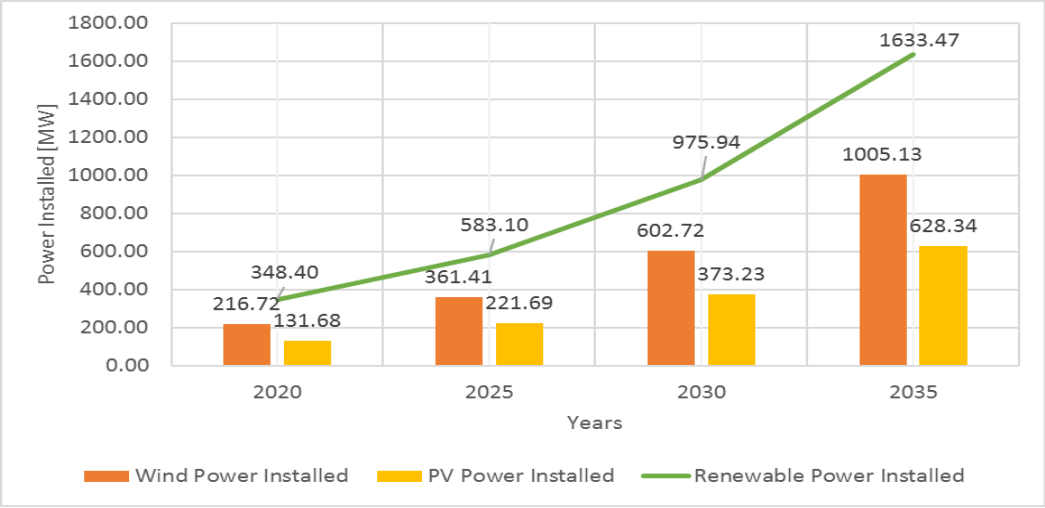

Figure 6. Power Growth of Renewables Energies [MW] in Scenario 2 – Green Plus.

Table 5 summarizes the increase in wind and photovoltaic potential for each scenario. In both scenarios, wind power has a higher growth than photovoltaic, this technology had more relevance in this study in both scenarios. The wind power is considered that would affect the storage of energy due to its stochastic generation. The growth of photovoltaic does not match that of wind onshore, however it was important to detail similar percentage growth to wind in the *Green Plus*, to understand its impact on the evolution

of the energy available to store in the case that the photovoltaic growth is similar percent that of wind onshore.

Table 5. Summary of Renewable Power installed in the proposed scenarios decomposed by type.

		2020	2025	2030	2035
Wind Power Available [MW]	*Scenario 1*	212.57	321.89	487.41	738.05
	Scenario 2	216.72	361.41	602.72	1005.13
Photovoltaic Power Available [MW]	*Scenario 1*	126.40	173.38	237.82	326.22
	Scenario 2	131.68	221.69	373.23	628.34

3.2. Definition of the study plant

A study plant was chosen to which the LAES system would be applied in each simulation of the scenarios proposed above, where this plant had a participation of the renewable energy grid, obtaining the injected and not into the grid in each scenario, being the available energy to storage. For this plant, the LAES system was applied in the representative years of each of the scenarios, according to the results obtained from the simulation, where its results and procedures will be detailed in *Section 5*.

The definition of the study plant was developed with a hub of representative renewable plants located in the south of Tenerife. From this hub, was chosen the renewable plants with the largest share of renewable energy at this site and belonging to the same owner. This was done with the information from Annuary Energy Book and GrafCan Viewer. The Study Plant and its power selected is detailed in *Table 6.*

Table 6. Details of the renewable energy plant of study.

System	Detail	Power Installed [MW]
Wind farms (Wind)		*44*
	Wind Farm 1	22
	Wind Farm 2	12
	Wind Farm 3	10
Photovoltaic Plants (PV)		*10*
	Photovoltaic Farm 1	10
Total in Study Plant (Wind + PV)		***54***

This study plant is expected to have the same power until 2035, causing its participation in the renewable injection will decrease as new generation plants enter, these being expected to grow the renewable potential in the proposed scenarios. Therefore, for this plant was proposed a LAES plant that would take advantage of the surplus of this energy.

4. LAES SYSTEM MODEL DEFINITION

To start modelling the Liquid Air Storage system to integrate in the study plant, first information was sought in the literature about plant design, performance characteristics, results to be expected among other functionality parameters. Initially the model was selected, where the variety of types of LAES system and the different efficiencies was analyzed, selecting the Kapitza cycle due the best theoretical results were obtained in this cycle compared with other cryogenic cycles [31]. Then defined the type of LAES, from the literature was taken as the basis to set the parameters of the plant model for

the project, proposing design of 2 plants of different size, where these parameters were made based on the literature found and the use of chemical process software.

4.1. Definition of LAES systems to integrate in the Scenarios

The two LAES systems that could be integrated in the study plant are defined in this section, detailing the power and energy that each system will have. The definition of these was realized in base of the reference data for modelling LAES storage system and the parameters obtained from the literature to develop the thermodynamic model [32]. The additionally information of the system was complete with the use of chemical process simulator. The types of proposed storage systems detailed in *Table 7* were chosen for the study plant.

Table 7. Definition of Liquid Air Energy Storage sizes for the study plant.

LAES Plant	Rated Electrical Power Output [MW]	Storage [MWh]	Load Time [h]	Download Time [h]
LAES 1	10	20	8	2
LAES 2	20	40	8	2

The design of the plants was developed according to estimates of the grid node, derived from calculation of its 2020 consignment [5]. The LAES 1 plant (10 MW/20 MWh) has been proposed for a conservative setpoint scenario such as *Green*, according to the installed renewable power of the node (*Table 6*). For LAES 2 (20 MW/40 MWh) it has been assumed for a scenario where the system operator's consignments are higher for the same grid node. This configuration doubles the charging and discharging power, as well as the storage capacity with respect to LAES 1. It should be noted that these storage capacities are designed specifically for the network node under study in this work, independently of the large-scale storage at island level (estimated at 200 MWh)

Detailing the charging time for the storage system, 8 hours was established for this parameter with a discharge time of 2 hours, where according to the literature, are the most used [33]. Additionally, this literature details other important parameters like pressure, temperature and RTE in LAES, therefore, this reference was the basis to begin with the development of the LAES plants used in this project.

Describing the functioning of the LAES system, the charge process is shown in *Figure 7*, where initially the cleaned air enters the system and is compressed with compressors (*C1 and C2*). In this process heat was generated and extracted with the system High Grade Warm Storage HGWS (*Red*). The compressed air in low temperature enters a Cold Box, in charge of reducing the air to cryogenic temperature, where the contribution of cold to perform the above is made by the system High Grade Cold Storage HGCS (*Blue*). Part of the flow of air is used to recover energy in the process with Cryoturbines (*CT1 and CT2*).

The air quality after the Cold Box was not completely liquid, for this reason a separator (*Sep*) was used to send the liquid air to the Liquid Air Tank Storage (*LAES Tank*), where the air in vapor phase is recirculated to obtain more air in the liquid phase. This recirculation flow is sent to the start of the cycle, with the objective to maintain the

[5] The setpoint values are internal company data of the owner of the renewables systems of the Study Plant.

temperature at the beginning of the charging process, increasing the performance of this process.

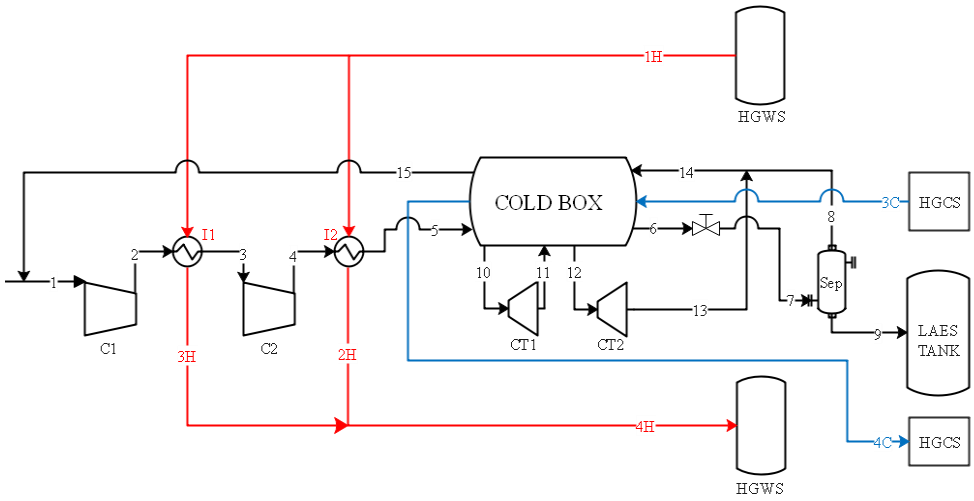

Figure 7. LAES Schematic system Charge Phase.

The discharge phase represented in *Figure 8*, where the air stored in the LAES Tank is sent to a Cryopump (*CP*), this process increases the pressure and obtains the possibility to extract the cold with the system HGCS for use in the charging process (*Blue*). The above is due the air to be at high temperatures to work in the turbines *T1*, *T2*, *T3* and *T4*, but the extract of cold is not sufficient to add the necessary heat to move these turbines, for this reason, in the process is added a heat share coming from HGWS (*Red*), obtained from the charge phase with the compressors. The air in high pressure and temperature provides the work to move the output turbines, being these 4 the ones that generate the electrical power to the system.

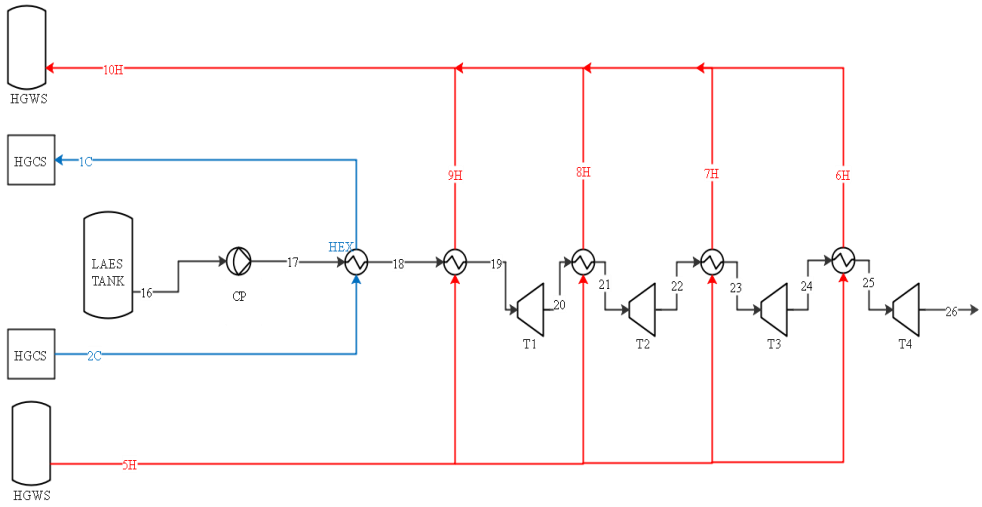

Figure 8. LAES Schematic system Discharge Phase.

To properly perform the entire charging and discharging process of the LAES systems established for this project, where the initial parameters are detailed in *Table 9*, these were taken from different references in the literature. With these values, the initial parameters for each LAES plant were defined to construct the proposed systems to use in the study plant for each scenario. However, to model a basic LAES system was necessary to add functional parameters, recommended from the reference [30] for apply

in the modelling maps for the same reference, where this additional information is detailed in *Table 8*.

Table 8. Parameters used for design of LAES plants.

Parameter	Unit	LAES 1	LAES 2
Rated power output	MW	10	20
Energy capacity	MW h	20	40
Nominal discharge time	H	2	2
Nominal charge time	H	8	8
Compressor isentropic efficiency [32]	%	89	89
Turbines isentropic efficiency [32],[33]	%	80	80
Cryoturbines isentropic efficiency [32]	%	80	80
Cryopumps isentropic efficiency [30]	%	80	80
Compressor, Turbines, Cryoturbines and Cryopumps mechanic efficiency [34]	%	90	90
Quality of Liquid Air (in Separator) [31]	-	0.1356	0.1356
Recirculation Fraction (Xrf) [17]	-	0.10-0.50	0.10-0.50

Table 9. Parameters selected for the performance maps of LAES plant in [30].

Parameter	Unit	LAES
Charge Pressure (P_{ch})	bar	50
Discharge Pressure (P_d)	bar	75
Storage Pressure (P_s)	bar	1.5
Utilization factor of HGCS (eta_{HGCS})	%	0,9
Utilization factor of HGWS (eta_{HWCS})	%	0,9

With the data established in *Table 8* and *Table 9*, the performance maps to design the complete LAES Plants for reference were used to find important parameters like the recirculation fraction (*Xrf)* in the separator, the specific consumption (*SC)*, the turbine inlet temperature (*TIT)* for the turbines *T1 to T4* and the specific production (*SP)*. This maps details that were the first literature that create a guide to design a LAES system obtaining approximately results using some data like specific pressures and temperature, for this reason, in this project were used obtaining the results of sizing of the LAES plant in the detail in *Table 10*.

Table 10. Parameters found on the performance maps for LAES plant in [30].

Parameter	Unit	LAES
Recirculation Fraction (Xrf)	-	0.38
Specific Consumption (SC)	KWh_e/Kg_{LA}	0.278
Temperature Inlet Turbine (TIT)	K	426.3
Specific Production (SP)	KWh_e/Kg_{LA}	0,0778
RTE	-	0.28

According to the parameters found in the maps detailed in *Table 10*, it is detailed that the parameter recirculation fraction that is not specific in the data of initial parameters of *Table 8* is defined, setting a value of 0.38. But other parametric values were not defined with the literature, in this case a basic software that simulates the LAES model was

necessary to apply. DWSIM was the freeware tool used in this project to develop the thermodynamic process in LAES, where the consumed power in the process of compression and temperatures in some points of the system were adjusted with this software.

4.2. LAES Plant elements

In this section details the results obtained for each of the proposed size types in section 4.1. The important elements that work in the LAES plant for each storage system proposed is shown in *Table 11*, where these elements were important to know because with this data it was possible for the project to know the cost of each element, resulting in an approximate cost of each LAES plant to start the economic study.

Table 11. Summary of the components in the proposed LAES systems.

Element	Unit	LAES 1 (10 MW/20 MWh)	LAES 2 (20 MW/40 MWh)
Compressor 1	kW_e	4095	8190
Compressor 2	kW_e	4857	9714
Cryoturbine 1	kW_e	295	590
Cryoturbine 2	kW_e	135	270
Cryopump	kW_e	423	845
Turbine 1	kW_e	2500	5000
Turbine 2	kW_e	2500	5000
Turbine 3	kW_e	2500	5000
Turbine 4	kW_e	2500	5000
HGCS tank	m^3	789	1579
HGWS tank	m^3	392	784
Tank LAES	m^3	294	588

5. SIMULATION OF LAES IN THE SCENARIOS

Having defined the simulation parameters of the scenarios, including the plant of study that will have the LAES system and the different sizes of LAES proposed, in this section will show the results of the energy generated, injected and probably to store by the study plant in all the scenarios proposed. With this information, an analysis of these energies was carried out to obtain a basis for the application of the LAES system in each scenario, defining the best LAES system for each scenario.

5.1. Energy Produced by Study Plant Alone in Scenarios

For each year in each scenario, the study plant would generate 133.25 GWh, with the largest amount coming from wind energy, 116.95 GWh and 16.3 GWh from photovoltaic. According to the established growth for these scenarios, the generation would be maintained but the injection of this energy would be reduced. For example, starting with the *Green Scenario* being the conservative, in 2025 there would be a 0.74% of the total energy that would not be injected and possible to store, where advancing in years, it reaches 2035 with almost 25% of energy not injected (*Figure 9*).

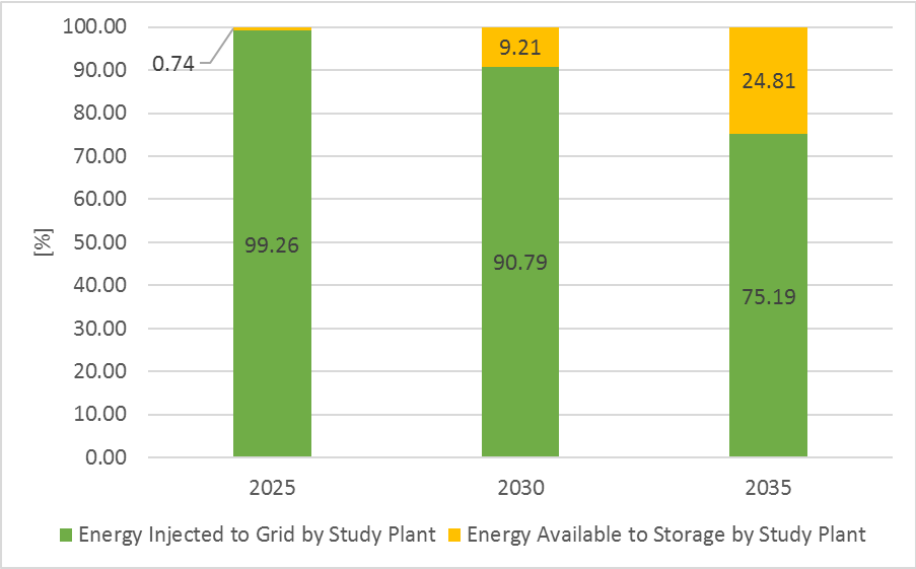

Figure 9. Green Scenario. Energy injected and available to storage by study plant in the representative years.

For the *Green Plus Scenario* with an excess of renewables with respect to the *Green Scenario*, it is detailed that from 2025 onwards the need for storage is present, where around 3,35 % (4,4 GWh) of the energy produced is not injected to the electrical grid. In the same scenario moving forward in the representative years, the need for storage becomes indispensable, with a 20% of the energy not injected in 2030 and increasing to 41% by 2035 (*Figure 10*). This means that a considerable growth in renewables would generate a saturation of the system, which even the grid-connected battery itself would not be able to support all the excess renewable energy generated.

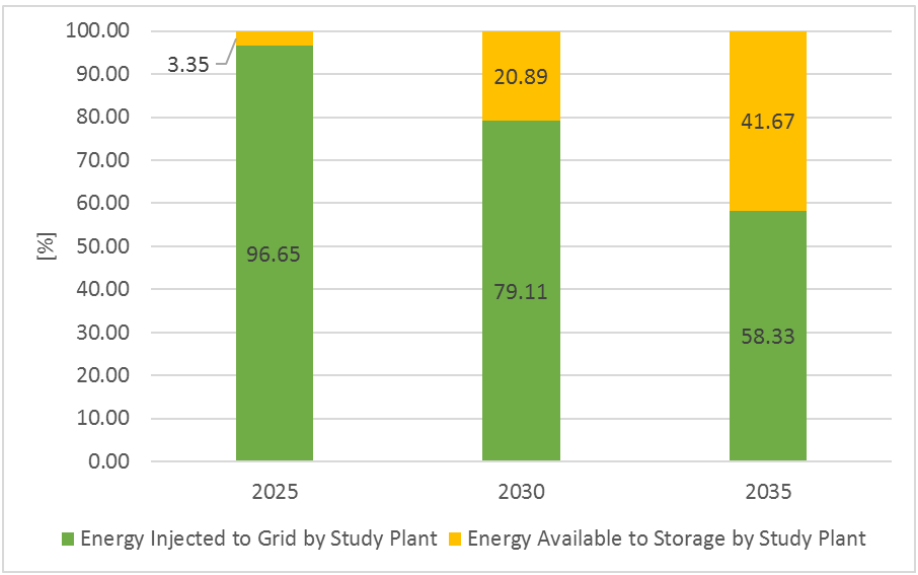

Figure 10. Green Plus Scenario. Energy injected and available to storage by study plant in the representative years.

5.2. LAES systems integrated with the Study Plant in the scenarios

With the information obtained from the scenario simulation, in this section is detailed the LAES plants that operate with the study plant for the representative years of the scenarios. This means that the simulation of the 2 LAES proposed in the previous chapters in each scenario was carried out if these systems were attached to the study

plant, operating in two ways: the first with the same restriction as the renewable energy from the study plant to inject energy in the grid (quick response); the second without restriction to grid injection for these batteries, approaching the not injected energy by the study plant completing up to 365 full discharge cycles per year or in the same way, as an annual reserve for the grid (reserve response).

The results are shown in terms of complete cycles per year, where the reason is that data could detailing how many times the battery would be fully charged and discharged energy to the grid. The above, represent the better way to see the effectiveness of the LAES system integrated with the Study Plant.

5.2.1. LAES 1 - 10 MW / 20 MWh

With the results obtained of the energy not injected in each of the scenarios, the LAES 1 with its 10 MW of power and 20 MWh storage, obtained working as quick response to 116 annual discharge cycles in the Green Scenario and 145 annual discharges cycles in the Green Plus Scenario. On the other hand, if this battery were to operate as an unrestricted reserve for grid network, it would achieve 365 full discharge cycles in the Green Scenario by the year 2035, while in the Green Plus Scenario it can complete this amount by 2030 (*Table 12)*.

Table 12. Completes cycles of discharge in the grid for LAES 1 (10 MW/20 MWh).

	Green Scenario			Green Plus Scenario		
Type	**2025**	**2030**	**2035**	**2025**	**2030**	**2035**
Quick Response [cycles over the year]	9	75	116	43	119	145
Reserve [cycles over the year]	9	75	365	43	365	365

The above results detail that the battery operating without restrictions as a reserve response has better possibilities to inject to the grid, working as a backup system which the grid operator would need to meet an annual quota of backup energy. Therefore, the LAES 1 battery for both scenarios, *Green* and *Green Plus* performs well if applied as a reserve response to be integrated with the study plant, with the year 2030 being the best year to install this size of battery.

5.2.2. LAES 2 - 20 MW / 40 MWh

The LAES 2 with 20 MW of power and 40 MWh of storage, the study was carried out working as a quick response and reserve response. If the system is operated as a quick response, the *Green Scenario* achieves a maximum of 86 complete discharge cycles, which is less than the *Green Plus Scenario*, which achieves up to 117. This shows that this system operating as a quick response is not technically viable (*Table 13*).

Table 13. Completes cycles of discharge in the grid for LAES 2 (20 MW/40 MWh).

	Green Scenario			Green Plus Scenario		
Type	**2025**	**2030**	**2035**	**2025**	**2030**	**2035**
Quick Response [cycles over the year]	4	53	86	21	87	117
Reserve [cycles over the year]	4	53	86	21	87	365

Detailing the obtained results of LAES 2, if these systems were to function as an annual reserve for the grid as reserve response, this system would achieve for the *Green Plus Scenario* up 365 full cycles. In contrast, in the *Green Scenario* the behavior of the battery would be similar in the two operations ways. Results suggest that a larger LAES storage does not mean a better use of the energy that is not injected by the study plant. According to the above, to obtain the better economic performance of the LAES systems integrated with Study Plant, the systems in Reserve Response were selected to elaborate the techno-economic analysis.

6. TECHNO-ECONOMIC ANALYSIS

This chapter begins by detailing the initial investment cost for each LAES system, where the calculation of these were taken from the literature. With this information and the results of the energy injected by each LAES system in section 5.2, operating as reserve response, the corresponding LCOE, IRR, NPV and Payback calculation were made for each of the representative years of the scenarios, taking account that the LAES system was integrated with the study plant [34].

The techno-economic results could be volatile with the LAES operating as a reserve, in addition to the lack of definition in the Spanish legislation of the selling energy price from batteries systems [35]. Due to the above, a sensitive study was carried out with respect to the cost of energy sales by this system, entering an addition to this cost in order to obtain better results. Finally, as a reserve the best energy injection results were obtained, in this document will show the economical results with the LAES with these results.

6.1. Cost of LAES Plants

For each plant, the initial investment costs were calculated according to the literature and obtaining the results in *Table 14* [36]. On one hand, it is detailed that the critical point of the initial cost of the LAES system is the compressors, where the cost per MW consumed/generated is higher compared to other components such as turbines. On the other hand, the importance of choosing the right HGCS and HGWS system, given that they provide heat energy for different phases of the system, which can be reduced if these contributions were from other systems as is the case with some LAES system integration proposals.

Table 14. LAES Investment Cost in Euro (€). Total and decomposed by element.

Element	LAES 1 (10 MW/20 MWh)	LAES 2 (20 MW/40 MWh)
Compressor 1	€ 1,165,858	€ 1,791,706
Compressor 2	€ 1,295,970	€ 1,991,724
Cryoturbine 1	€ 93,639	€ 164,169
Cryoturbine 2	€ 49,668	€ 87,079
Cryopump	€ 173,503	€ 346,971
Turbine 1	€ 528,618	€ 926,781
Turbine 2	€ 528,618	€ 926,781
Turbine 3	€ 528,618	€ 926,781
Turbine 4	€ 528,618	€ 926,781
HGCS tank	€ 214,695	€ 429,389
HGWS tank	€ 140,995	€ 281,988
Tank LAES	€ 79,986	€ 159,972
Approximate total cost	**€ 5,328,785**	**€ 8,960,120**

With the initial cost of a LAES battery, the calculation of LCOE and economic metrics that would define the economic viability of these systems integrated with renewable energy plants was carried out. To complement the above information, these calculations would require the installed power cost of wind onshore and photovoltaic for the study plant, using the values of 1050 USD/KW (892.5 €/KW[6]) for wind and 974 USD/KW (828.75 €/KW) for photovoltaic energy [17].

6.2. LCOE

Since the interest of the project was to know the technical-economic viability of the LAES systems integrated with a study plant, the calculation of this parameter was carried out considering the energy of both, the study plant and that provided by the LAES. This to know the cost of the energy that an integral Study Plant + LAES system should consider obtaining the best economic results. With the data obtained from *Section 5,* using the LAES plant as reserve response, the calculation of the proposed LCOE was carried out.

According to the data obtained and detailed in *Table 15*, for both the *Green Scenario* and the *Green Plus Scenario*, the best result in the application of battery in study plant was obtained from the LAES 1 (10 MW/20 MWh) with an average value of 50,80 €/MWh for the first Scenario and 58.12 €/MWh to the second. However, it should be noted that the values obtained with respect to the LAES 2 (20 MW/40MWh) is 2 to 4 €/MWh lower, for which, if the battery were to carry out the same number of annual discharges or complete cycles as LAES 1, it would be possible to obtain higher income with the LAES 2. Comparing these batteries with the Study Plant working without storage systems, it is highlighted that the integration of these batteries increases the cost around 3-6 €/MWh the LCOE.

Table 15. LCOE average result for the simulated scenarios with LAES working as reserve.

System	Unit	Green	Green Plus
Study Plant	*€/MWh*	47.90	55.90
Study Plant + LAES 1 (10 MW/20MWh)	*€/MWh*	50.80	58.12
Study Plant + LAES 2 (20 MW/40MWh)	*€/MWh*	53.61	61.34

6.3. NPV, IRR and Payback

For the calculation of these economic metrics that would define the viability or not of the application of LAES systems integrated with the study plant, the initial parameters to the economic evaluation are detailed in *Table 16*. With the objective to define the initial conditions for each economic study that would be carried out in each scenario for the Study Plant + LAES, adjusting to the most appropriate to develop the study.

Table 16. Parameters in the economic calculation of NPV, IRR and Payback.

Parameter	Unit	Value	Reference
Annual reduction in production	*%*	1.00	-
Annual reduction in wind investment cost	*%*	5.00	IRENA [37]
Annual reduction in photovoltaic investment cost	*%*	10.00	IRENA [37]

[6] Exchange rate used 1 USD = 0.85 €

Annual reduction in LAES investment cost	*%*	2.00	-
Opportunity cost	*%*	8.00	[38]
Project life cycle	*Years*	25	[38]
Discount rate	*%*	8.00	[39]
Amortization period	*Years*	15	-
Cost of energy	*€/MWh*	47.68	OMIE [40]
Annual reduction in cost of energy	*%*	1.00	-

Because the cost of energy sold at grid would have a negative evolution according to the historical data of OMIE, a sensitive study was carried out for the cost of energy from the LAES system integrated to the Study Plant, adding 15 €/MWh by 15 €/MWh up to 60 €/MWh in the cost of energy sold by the battery and obtaining the minimum aggregate to get the better results in each scenario. The cost of the energy supplied to the grid by the renewables of the Study Plant will not be applied to this sensitive study, because these energies have a cost regulation defined by Spanish decrees.

In addition to the search for the feasibility of the Study Plant + LAES systems, results were obtained first with the Study Plant without the battery, these data being the comparative base with respect to the results obtained with the sensitivity analysis of the Study Plant + LAES system. Starting with the results of the Study Plant, the *Table 17* shows in the *Green Scenario* that the study plant achieves better results than the Green *Plus Scenario* (*Table 18)*, due to the large amount of energy that is wasted in the *Green Plus* as the electricity grid has more renewable energy producers. Highlight that for *Green Scenario*, even with energy loss, the study plant would still be profitable to operate.

Table 17. Results of NPV, IRR and Payback of Study Plant in Green Scenario.

		Green Scenario		
	Unit	**2025**	**2030**	**2035**
NPV	€	5,250,806.15	7,004,152.20	3,793,500.09
IRR	%	10.06	11.64	10.68
Payback	Years	15	12	13

In contrast, the *Green Plus Scenario* details in *Table 18* that the study plant in 2035 would not achieve satisfactory results, because only the 59% of the energy produced would be injected to the grid, being the other part a considerable economic loss that is reflected in a negative NPV, a low IRR percentage and the impossibility of recovering the investment in less than 25 years.

Table 18. Results of NPV, IRR and Payback of Study Plant in Green Plus Scenario.

		Green Plus Scenario		
	Unit	**2025**	**2030**	**2035**
NPV	€	3,921,926.19	1,359,918.58	-3,953,851.32
IRR	%	9.55	8.73	4.95
Payback	Years	16	19	>25

With the above results for the study plant in the scenarios, the corresponding economical metrics was obtained for the integral systems of Study Plant + LAES, where the sensitive analysis proposed to the selling price of the energy injected by the LAES would give better results. The results were compared to the base results of the study plant to know how to affect the integration of the LAES 1 (10 MW/20 MWh) and 2 (20 MW/40 MWh) with the study plant, for this a comparison was made between the best IRR results from the integrated system in each scenario with the obtained in the *Tables 19* and *20*.

The results of the integration of the batteries with the study plant is shown in Figure *11*, detailing the IRR results obtained in the *Green Scenario* with Study Plant + LAES 1 (10 MW/20 MWh). For this system, in 2025 details that adding an aggregate to the cost of sale energy of LAES does not make much difference in the IRR. However, from 2030 onwards the increase in selling price shows a clear difference between each IRR value, being more noticeable in 2035.

Figure 11. IRR Green Scenario with Study Plant + LAES 1 (10 MW/ 20MWh), Reserve Mode, with sensitive analysis in the selling price of energy from LAES system.

For Study Plant + LAES 2, the IRR for the *Green Plus Scenario* is detailed in *Figure 12*, where in comparison to Study Plant + LAES 1, the first performed better in a high growth of renewables of Green Plus Scenario. It is shown that only in the year 2030, more than the cost of opportunity (8%) is obtained from an addition to the energy selling price of the LAES battery of 30 €/MWh. Detailed that the sale price of energy from the liquid air battery greatly affects the benefits that could be obtained, in a moderate level of insertion of renewables as is the *Green Scenario*, a LAES 1 (10 MW/ 20 MWh) system would not need additions to the sale price of energy, where compared to LAES 2 (20 MW/ 40 MWh), this is not achieved until 2030 in the *Green Plus Scenario*.

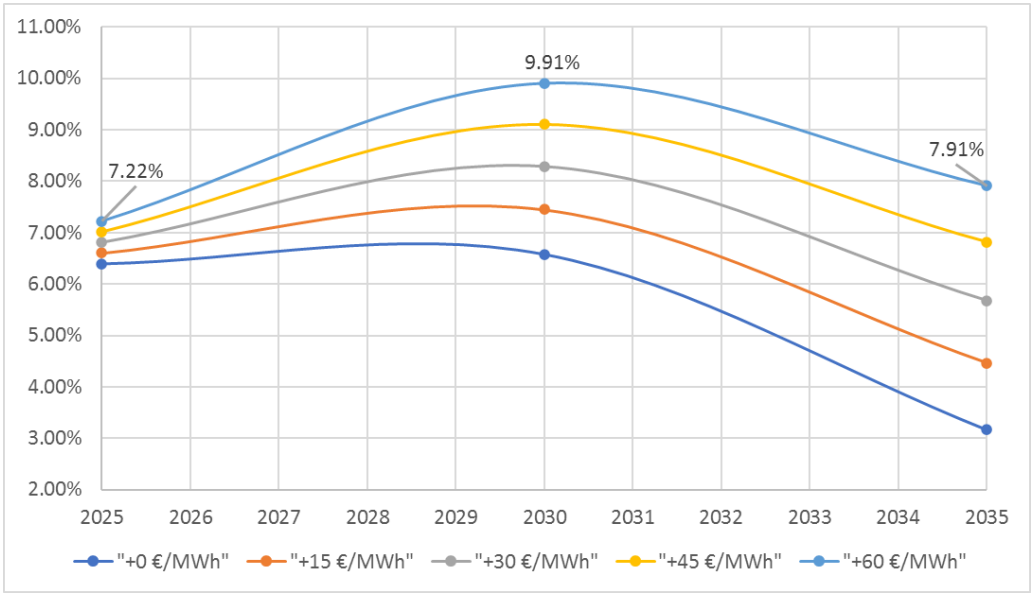

Figure 12. IRR Green Plus Scenario with Study Plant + LAES 2 (20 MW/ 40MWh), Reserve Mode, with sensitive analysis in the selling price of energy from LAES system

To better compare between scenarios, for the *Green* the integration of LAES with the study plant operating as a reserve would not require an addition to the selling price of energy. For the *Green Plus Scenario*, only the year 2030 would be feasible to implement the integrated systems and it would be necessary to apply an addition greater than 30 €/MWh to the selling price of the energy form the LAES battery.

The *Tables 19* and *20* shows the best results choice for each Study Plant + LAES system, with the maximum addition of 60 €/MWh to the selling price of energy from the battery. The economic metrics for the application of this system in the *Green Scenario* are optimistic, where compared to those obtained for the study plant alone, having similar values to those for 2030 and 2035. With respect to the *Green Plus Scenario*, only 2030 is it possible to apply LAES systems, where the better results are obtained compared to the study plant alone, although with a difference of a higher Payback.

Table 19. Best economical results for Study Plant + LAES 1 (+60 €/MWh in cost of energy sold).

	NPV [€]	IRR [%]	Payback [Years]
Green Scenario – 2030	8,009,115.22	11.52	12
Green Plus Scenario – 2030	2,364,881.61	9.07	18

Table 20. Best economical results for Study Plant + LAES 2 (+60 €/MWh in cost of energy sold).

	NPV [€]	IRR [%]	Payback [Years]
Green Scenario – 2035	7,578,931.86	11.84	13
Green Plus Scenario – 2030	4,713,056.13	9.91	16

7. CONCLUSIONS

The LAES systems are technical and economic feasible to apply in Tenerife as a storage system integrated with renewable energy, in a configuration as reserve energy for the grid and with incentives applied to the cost of selling power from the battery. Additionally,

these systems have a constant technological evolution, reduced use of space, with a foresight in the reduction of its investment cost due the use of industry technologies, this making it possible to obtain better profits compared to other storage systems and facilitating its successful introduction in islands.

The lack of normative to develop these technologies in Spain has not allowed a greater implementation of these systems, in both island and non-island territories. If clear regulations are established with the basis of operation, the cost of energy for these batteries and others in Tenerife electricity grid, results of greater interest and complementary to the results obtained in this project would be achieved, improving the integration of storage systems in the face of a massive growth of renewables.

The cost of energy sale has an important impact on the economic results of the LAES battery, where it was highlighted that it is necessary for these storage systems to have an evolution of the cost of energy sale to generate positive incomes. To obtain the total potential of LAES technologies, it would be necessary to develop an in-depth study with the systems, conducting sensitive studies with other electricity market factors such as, remuneration in energy delivery, loans, among others.

Expansion of the literature

LAES plants developed in the literature have some characteristics that could increase the efficiency. One of these is a minimum of 200°C at the outlet of the systems in the turbines, whereas a plant of less than 50 MW was found in this literature to obtain better RTE. Therefore, this was taken as the average contribution of external energy in the discharge phase for HGWS to the Turbines to obtain better results [39].

In the networked scope of application for economic analysis, one must consider how the system LAES would operate in a network. According to a study in the UK, revenues are more stable when the system works only as an arbitration system, if it is used for combined actions such as quick response and reserve, revenues are more volatile [35].

Spain has a precedent of a techno-economic study of an LAES system connected to the peninsular electric grid, used in this research; where with the use of a 100 MW plant of this technology, the LCOE and LCOS was 250 €/MWh and 150 €/MWh respectively [38]. The above literature concluded that it is not necessary to implement a big size of LAES plant to obtain better LCOE.

Bibliography

[1] M. Miguel, T. Nogueira, and F. Martins, “Energy storage for renewable energy integration: The case of Madeira Island, Portugal,” in *Energy Procedia*, 2017, vol. 136, pp. 251–257, doi: 10.1016/j.egypro.2017.10.277.

[2] G. de Canarias, “Anuario Energético de Canarias 2019,” 2019.

[3] A. Ramirez-Diaz, F. J. Ramos-Real, and G. A. Marrero, “Complementarity of electric vehicles and pumped-hydro as energy storage in small isolated energy systems: case of La Palma, Canary Islands,” *J. Mod. Power Syst. Clean Energy*, vol. 4, no. 4, pp. 604–614, Oct. 2016, doi: 10.1007/s40565-016-0243-2.

[4] D. H. Alamo *et al.*, “An Advanced Forecasting System for the Optimum Energy Management of Island Microgrids,” in *Energy Procedia*, 2019, vol. 159, pp. 111–116, doi: 10.1016/j.egypro.2018.12.027.

[5] O. R. Llerena-Pizarro, R. P. Micena, C. E. Tuna, and J. L. Silveira, “Electricity sector in the Galapagos Islands: Current status, renewable sources, and hybrid

power generation system proposal," *Renew. Sustain. Energy Rev.*, vol. 108, no. July 2018, pp. 65–75, 2019, doi: 10.1016/j.rser.2019.03.043.

[6] S. Mazzoni, S. Ooi, B. Nastasi, and A. Romagnoli, "Energy storage technologies as techno-economic parameters for master-planning and optimal dispatch in smart multi energy systems," *Appl. Energy*, vol. 254, no. August, p. 113682, 2019, doi: 10.1016/j.apenergy.2019.113682.

[7] Lazard, "Levelized Cost of Storage Analysis - Version v6.0," 2020.

[8] O. Schmidt, S. Melchior, A. Hawkes, and I. Staffell, "Projecting the Future Levelized Cost of Electricity Storage Technologies," *Joule*, vol. 3, no. 1, pp. 81–100, Jan. 2019, doi: 10.1016/j.joule.2018.12.008.

[9] S. Mazzoni, S. Ooi, A. Tafone, E. Borri, G. Comodi, and A. Romagnoli, "Liquid Air Energy Storage as a polygeneration system to solve the unit commitment and economic dispatch problems in micro-grids applications," in *Energy Procedia*, Feb. 2019, vol. 158, pp. 5026–5033, doi: 10.1016/j.egypro.2019.01.660.

[10] G. Comodi, F. Carducci, J. Y. Sze, N. Balamurugan, and A. Romagnoli, "Storing energy for cooling demand management in tropical climates: A techno-economic comparison between different energy storage technologies," *Energy*, vol. 121, pp. 676–694, Feb. 2017, doi: 10.1016/j.energy.2017.01.038.

[11] C. Damak, D. Leducq, H. M. Hoang, D. Negro, and A. Delahaye, "Liquid Air Energy Storage (LAES) as a large-scale storage technology for renewable energy integration – A review of investigation studies and near perspectives of LAES," *Int. J. Refrig.*, vol. 110, pp. 208–218, Feb. 2020, doi: 10.1016/j.ijrefrig.2019.11.009.

[12] R. Morgan, S. Nelmes, E. Gibson, and G. Brett, "Liquid air energy storage - Analysis and first results from a pilot scale demonstration plant," *Appl. Energy*, vol. 137, pp. 845–853, 2015, doi: 10.1016/j.apenergy.2014.07.109.

[13] J. Kim, Y. Noh, and D. Chang, "Storage system for distributed-energy generation using liquid air combined with liquefied natural gas," *Appl. Energy*, vol. 212, pp. 1417–1432, Feb. 2018, doi: 10.1016/j.apenergy.2017.12.092.

[14] J. Kim and D. Chang, "Pressurized cryogenic air energy storage for efficiency improvement of liquid air energy storage," in *Energy Procedia*, Feb. 2019, vol. 158, pp. 5086–5091, doi: 10.1016/j.egypro.2019.01.638.

[15] Cabildo de Tenerife, "Espacios Naturales Protegidos - Plan Insular de Ordenación de Tenerife 2011," 2011. Accessed: Apr. 29, 2020. [Online]. Available: https://www.tenerife.es/planes/PIOT/adjuntos/ADef_E-Base_Puertos_Feb2011_11.pdf.

[16] J. Mendoza Aguilar, F. J. Ramos-Real, and A. J. Ramírez-Díaz, "Improving Indicators for Comparing Energy Poverty in the Canary Islands and Spain," *Energies*, vol. 12, no. 11, p. 2135, Jun. 2019, doi: 10.3390/en12112135.

[17] Lazard, "Levelized Cost of Energy - Version 14.0," 2020. [Online]. Available: https://www.lazard.com/media/451419/lazards-levelized-cost-of-energy-version-140.pdf.

[18] G. Frydrychowicz-Jastrzębska, "El Hierro Renewable Energy Hybrid System: A Tough Compromise," *Energies*, vol. 11, no. 10, p. 2812, Oct. 2018, doi: 10.3390/en11102812.

[19] F. J. Ramos-Real, J. Barrera-Santana, A. Ramírez-Díaz, and Y. Perez,

"Interconnecting isolated electrical systems. The case of Canary Islands," *Energy Strateg. Rev.*, vol. 22, pp. 37–46, Nov. 2018, doi: 10.1016/j.esr.2018.08.004.

[20] Red Eléctrica de España, "Red Eléctrica de España - Actividades." https://www.ree.es/es/actividades (accessed Jul. 13, 2020).

[21] Operador del Mercado Ibérico de Energía, "OMIE - Funciones." https://www.omie.es/es/funciones (accessed Jul. 13, 2020).

[22] Gobierno de España, *Real Decreto 738/2015, de 31 de julio, por el que se regula la actividad de producción de energía eléctrica y el procedimiento de despacho en los sistemas eléctricos de los territorios no peninsulares*. 2015.

[23] R. Guerrero-Lemus, B. González-Díaz, G. Ríos, and R. N. Dib, "Study of the new Spanish legislation applied to an insular system that has achieved grid parity on PV and wind energy," *Renew. Sustain. Energy Rev.*, vol. 49, pp. 426–436, Sep. 2015, doi: 10.1016/j.rser.2015.04.079.

[24] D. G. de P. E. y Minas, "Resolución de 30 de junio de 2017," 2017.

[25] R. E. de España, "Demanda de energía eléctrica en tiempo real, estructura de generación y emisiones de CO2." https://demanda.ree.es/visiona/home (accessed Jul. 13, 2020).

[26] G. de Canarias, "IDECanarias visor 4.5.1." https://visor.grafcan.es/visorweb/ (accessed Jun. 19, 2020).

[27] Ministerio para la Transición Ecológica el Reto Demográfico, "Plan Nacional Integrado de Energía y Clima 2021-2030," 2021.

[28] A. R. Díaz, F. J. Ramos-Real, G. A. Marrero, and Y. Perez, "Impact of electric vehicles as distributed energy storage in isolated systems: The case of tenerife," *Sustain.*, vol. 7, no. 11, pp. 15152–15178, 2015, doi: 10.3390/su71115152.

[29] G. A. Marrero, Y. Perez, M. Petit, and F. J. R. Real, "Electric vehicle fleet contributions for isolated systems. The case of the Canary Islands," *Int. J. Automot. Technol. Manag.*, vol. 15, no. 2, p. 171, 2015, doi: 10.1504/IJATM.2015.068552.

[30] Gobierno de España, *Real Decreto-ley 23/2020 de 23 de junio*. 2020.

[31] S. Hamdy, F. Moser, T. Morosuk, and G. Tsatsaronis, "Exergy-based and economic evaluation of liquefaction processes for cryogenics energy storage," *Energies*, vol. 12, no. 3, p. 493, Feb. 2019, doi: 10.3390/en12030493.

[32] A. Tafone, A. Romagnoli, E. Borri, and G. Comodi, "New parametric performance maps for a novel sizing and selection methodology of a Liquid Air Energy Storage system," *Appl. Energy*, vol. 250, pp. 1641–1656, Sep. 2019, doi: 10.1016/j.apenergy.2019.04.171.

[33] A. Sciacovelli, A. Vecchi, and Y. Ding, "Liquid air energy storage (LAES) with packed bed cold thermal storage – From component to system level performance through dynamic modelling," *Appl. Energy*, vol. 190, pp. 84–98, Mar. 2017, doi: 10.1016/j.apenergy.2016.12.118.

[34] A. Tafone, Y. Ding, Y. Li, C. Xie, and A. Romagnoli, "Levelised Cost of Storage (LCOS) analysis of liquid air energy storage system integrated with Organic Rankine Cycle," *Energy*, vol. 198, p. 117275, May 2020, doi: 10.1016/j.energy.2020.117275.

[35] A. Vecchi, Y. Li, P. Mancarella, and A. Sciacovelli, "Integrated techno-economic

assessment of Liquid Air Energy Storage (LAES) under off-design conditions: Links between provision of market services and thermodynamic performance," *Appl. Energy*, vol. 262, p. 114589, Mar. 2020, doi: 10.1016/j.apenergy.2020.114589.

[36] S. Wu, C. Zhou, E. Doroodchi, and B. Moghtaderi, "Techno-economic analysis of an integrated liquid air and thermochemical energy storage system," *Energy Convers. Manag.*, vol. 205, p. 112341, Feb. 2020, doi: 10.1016/j.enconman.2019.112341.

[37] IRENA, *Renewable Power Generation Costs in 2019*. 2019.

[38] M. Legrand, L. Miguel Rodríguez-Ant, C. Martinez-Arevalo, and F. Guti Errez-Martín, "Integration of liquid air energy storage into the spanish power grid," *Energy*, vol. 187, 2019, doi: 10.1016/j.energy.2019.115965.

[39] C. Xie, Y. Hong, Y. Ding, Y. Li, and J. Radcliffe, "An economic feasibility assessment of decoupled energy storage in the UK: With liquid air energy storage as a case study," *Appl. Energy*, vol. 225, pp. 244–257, Sep. 2018, doi: 10.1016/j.apenergy.2018.04.074.

[40] OMIE, "Evolución del mercado de electricidad - Informe Anual," 2020. [Online]. Available: https://www.omie.es/sites/default/files/2020-02/informe_anual_2019_es.pdf.

[41] L. Guo, Z. Gao, W. Ji, H. Xu, L. Chen, and J. Wang, "Thermodynamics and Economics of Different Asymmetric Cold Energy Transfer in a Liquid Air Energy Storage System," *Energy Technol.*, vol. 8, no. 5, p. 1901487, May 2020, doi: 10.1002/ente.201901487.

[42] Y. Ding, L. Tong, P. Zhang, Y. Li, J. Radcliffe, and L. Wang, "Chapter 9: Liquid Air Energy Storage," in *Storing Energy*, Elsevier Inc., 2016, pp. 167–181.

APPENDIX

1. Detailed definition of Scenarios

1.1. Green Scenario

Table 1. Wind and PV installed and processed power Green Scenario.

Technology	Value [MW]
Wind Power Installed 2019	195.645
Photovoltaic Power Installed 2019	118.654
Wind Power to grid Processed	252.950
Photovoltaic Power to grid Processed	52.300
Wind Power installed prospected in 2029	**448.595**
Photovoltaic Power installed prospected in 2029	**223.254**

For this scenario, the processed potential of wind power in 2029 would be installed, however, for photovoltaic being a technology that in reduced year has reduced its price [37], it is anticipated that by 2029, twice the potential of the prospective network could be installed. It should be noted that the photovoltaic power projected for 2029 would be that connected to the grid and processed for generation by companies dedicated to the electricity generation sector, for this reason, systems such as self-consumption or installations by companies outside this sector are not included.

The calculation for this scenario were made as follows:

1) By 2029, the total wind and solar power would be the sum of the installed in 2018 available in 2019 plus the processed in February 2020, where the *equation 1* and *2* represent the operation for each technology.

$$P_{w,2029} = \sum_{1}^{n} P_{w,n,2019} + \sum_{1}^{n} P_{w,n,p} \quad (1)$$

$$P_{pv,2029} = \sum_{1}^{n} P_{pv,n,2019} + 2 * \sum_{1}^{n} P_{pv,n,p} \quad (2)$$

Where the sub index *w* and *pv* represent wind and photovoltaic respectively, *n* is the number of plants for each technology and *p* represents the processed power. The total of renewable power in 2029 would be represented by the *equation 3*, being the sum of wind and power.

$$P_{Renewable,2029} = P_{w,2029} + P_{pv,2029} \quad (3)$$

2) Having obtained the target value for wind and photovoltaic power in 2029, the percentage growth of these powers from the year 2019 was found. This percentage was calculated with the help of the formula of the compound annual growth rate *C*, which allows to find the percentage growth between year of renewable power, where is adapted to this project in the *equation 4* for photovoltaic power and *equation 5* for wind power.

$$C_{pv} = \left(\frac{P_{pv,2029}}{P_{pv,2019}}\right)^{1/(2029-2019)} - 1 \quad (4)$$

$$C_{wind} = \left(\frac{P_{w,2029}}{P_{w,2019}}\right)^{1/(2029-2019)} - 1 \quad (5)$$

The results of growth using the *equation 4* and *5* are detailed in *Table 2* below.

Table 2. Growth of Renewables Power in Green Scenario.

Renewable Energy	Growth [%]
Wind	8.65
Photovoltaic	6.52

1.2. Green Plus Scenario

In this Scenario, the growth of wind and photovoltaic renewable potential is based on th objective of PNIEC, specifically the coverage of 74% of energy demand by renewable generation. Starting with the electrical demand in 2019, which was 3546,84 GWh on Tenerife which the renewable potential in *Table 1*, a contribution to the grid of these energies of 692,56 GWh was obtained, which is approximately 19,70%. Assuming that energy demand would be maintained in 2030, the 74% coverage for the same year would be 2624,66 GWh. With the above, it was assumed that both wind and photovoltaic would have an equal share, meaning each would cover 50% of the energy, thus obtaining the results in *Table 3.*

Table 3. Proposed Share of Renewable in Tenerife year 2030.

Renewable Generation in 2030	GWh	%
Wind	1312.33	50
PV	1312.33	50
Total	**2624.66**	**100**

With the amount of energy that each renewable must cover from the energy demand, it was possible to obtain the approximate power need to cover that demand per year. For this, the load factor represented in the *equation 6* was applied, where was necessary to know the quantity of operating hour of each renewable technology.

$$F_c(h) = \frac{E_{annual}}{P_{nom}} \quad (6)$$

To calculate the number of operating hours of the load factor of each renewable technology in 2030, an average of the load factor of the years before 2019 was obtained from the Energy Yearbook, detailed that data in *Table 4* and *Table 5* for wind and photovoltaic energy, respectively. The result of this average is applied in *equation 8* for each technology, finding the expected power that covers that energy.

Table 4. History of the available of Wind Energy in Tenerife.

Year	Available Hours Wind in the Year - Fc [hours]	Available Wind [%]
2015	2062	23.54
2016	1931	22.04
2017	1847	21.08
2018	2482	28.33
2019	2556	29.18
Mean	**2175.6**	**24.84**

Table 5. History of the available of Photovoltaic Energy in Tenerife.

Year	Available Hours Photovoltaic in the Year - Fc [hours]	Available Photovoltaic [%]
2010	1701	19.42
2011	1651	18.85
2012	1525	17.41
2013	1676	19.13
2014	1647	18.80
2015	1616	18.45
2016	1619	18.48
2017	1617	18.46
2018	1605	18.32
2019	1634	18.65
Mean	**1629.1**	**18.60**

With the data obtained from the average wind and photovoltaic operating hours detailed in *Tables 4* and *5*, clearing the load factor of *equation 7*, the nominal power required to achieve the estimated energy production in 2030 was obtained with the help of the available hours prospect in 2030. The growth of renewable power for photovoltaic and wind was obtained applying the formula of compound annual growth rate, development in the scenario 1 and detailed from this scenario in the *equation 9*. Given that 2030 would be the targets to cover the energy, but in the simulation the renewable energy is restricted to 70%, the percentage growth of renewable power was reduced. The result for the island of Tenerife is a growth is detailed in *Table 6*.

$$C_{ren} = \left(\frac{P_{ren,2300}}{P_{ren,2018}}\right)^{\left(\frac{1}{2030-2018}\right)} - 1 \quad (7)$$

Table 6. Growth of Renewables Power in Green Scenario.

Renewable Energy	Growth [%]
Wind	10,78
Photovoltaic	10,98

2. Detailed definition of LAES system

2.1. Liquid air storage tank

Table 7. Base parameters to LAES design.

Parameter	Unit	LAES
Recirculation Fraction (Xrf)	-	0.38
Specific Consumption (SC)	KWh_e/Kg_{LA}	0.278
Temperature Inlet Turbine (TIT)	K	426.3
Specific Production (SP)	KWh_e/Kg_{LA}	0,0778
RTE	-	0.28

With the data obtained from *Table 7*, it was possible to obtain sizes and flows of the liquid air storage tank, this with the specific consumption and production. The above parameters are referenced to the liquid air Flow at the entrance and exit of the LAES tank, therefore, by this means it was possible to know the necessary exit and entrance flows, by means of the following equations:

$$SP = \frac{P_d}{\dot{m}_{LA,d}} = \frac{P_c - P_{ct}}{\dot{m}_{LA,d}} \quad (8)$$

$$SC = \frac{P_l}{\dot{m}_{LA,l}} = \frac{P_t - P_p}{\dot{m}_{LA,l}} \quad (9)$$

Where P_d refers to the electrical discharge power of the system, P_l to the electrical charge power, where P_c, P_{ct}, P_t y P_b correspond to the compressor, cryoturbine, turbine and pump power, respectively. The term $\dot{m}_{LA,d}$ means the mass flow liquid air after the storage tank y $\dot{m}_{LA,l}$ measn the mass flow of liquid air before the storage tank. Knowing the discharge electrical power to be obtained for each one of the systems, 10 and 20 MW respectively, the discharge mass flow is cleared from equation 10 of specific production, obtaining the results of *Table 8* for each plant size. It is clarified that for the calculation of the flow, the cryopump power was disregarded since it is relatively low. However, in the same section, it Will be detailed that the power of this cryopump for each plant does not reach 5% of the output power.

Table 8. Mass flow of download for each LAES system.

Parameter	Unit	LAES 1	LAES 2
Mass Flow of Download ($\dot{m}_{LA,d}$)	Kg/s	35.70	71.40

According to load time and energy storage capacity set from each system, the size of cryogenic storage tank was calculated, where with the use of *equation 10* the size in weight that the liquid air would occupy for each system was found.

$$Storage_{LA,tank} = t_d * \dot{m}_{LA,d} = t_l * \dot{m}_{LA,l} \quad (10)$$

Form the above equation, t_d is the download time and t_l is the load time for each plant. With the above, the size in weight of storage tank was calculated, yet this liquid air was in gross weight that the tank would support, therefore, the size of LAES tank was over dimensioned in storage in weight at the nearest multiple of 50. Detailed in parentheses in *Table 9*, the real occupation of liquid air was described and out, the size in actual weight of the storage tank.

Table 9. Mass flow of download for each LAES system.

Parameter	Unit	LAES 1	LAES 2
Storage (in weight)	ton	300 (257.069)	550 (514.138)

The calculated values were estimated, whereby means of a thermodynamic process simulation tool called DWSIM, it was later verified that these values were close to those estimated by the tool, therefore, these proposed values are those used for the general dimensioning of each the systems. Continuing with *equation 10* used for the LAES tank size, this same equation it was possible to obtain the system load mass flow, where the results are detailed in *Table 10*.

Table 10. Mass flow of Load for each LAES system.

Parameter	Unit	LAES 1	LAES 2
Mass Flow of Load ($\dot{m}_{LA}$)	Kg/s	8.92	17.852

With the previous process, flows and weights of the tanks where the air would be stored in cryogenic state were found. However, the size of the LAES tank with respect to weight was not sufficient to define some design and economic parameters, since it is also essential to know the volume of the liquid air that would occupy that among by weight. For the above and with the help of the CoolProp library, it was established that the density of the liquid air in cryogenic state, where the value found was 874.19 kg/m^3 (at temperature of 79.6 K and a pressure of 1.10 bar), obtaining with the previous value, the *equation 11* and the data in *Table 10*, the volume that the liquid air in the tank would occupy, summarized in *Table 11*.

$$V = \frac{m_{LA,Tank}}{\rho_{LA}} \tag{11}$$

Table 11. Volumetric Size for each LAES system.

Parameter	Unit	LAES 1	LAES 2
Storage (in volume)	m^3	320 (269.156)	600 (588.131)

With the above results, the *Table 12* summarizes the initial complementary conditions for each size of LAEs plant, where these values were used in the process of defining the system elements and system mass flow, all of this with the help of the DWSIM simulation tool.

Table 12. Complementary information for each LAES system.

Parameter	Unit	LAES 1	LAES 2
Rated power output	MW	10	20
Energy capacity	MWh	20	40
Nominal discharge time	H	2	2
Nominal charge time	h	8	8
Size of LAES tank (weight)	Ton	300	550
Size of LAES tank (volume)	m^3	320	600
Specific Consumption (SC)	KWh_e/Kg_{LA}	0.278	0.278
Specific Production (SP)	KWh_e/Kg_{LA}	0,0778	0,0778
Recirculation Fraction (Xrf) [36]	-	0.38	0.38
TIT	K	426.33	426.33

2.2. Mass flow in LAES system

Once the initial parameters for storage were fully defined, the rest of systems flows were defined, which was based on the same flow distribution as the reference [34]. These flows were necessary to calculated in the DWSIM tool, the generated and consumed power in each element of the system.

2.2.1. Mass flow in charge stage

Based on the load flow in the liquid air storage tank, the calculation of the mas flow was made to the previous point of the system, taking into account the values of the recirculation fraction in *Table 12* and the quality of the separation in *Table 7*. To know the mass flow before the separator, *equation 12* was used with the separation quality value of 0.1356 (liquid air fraction in gas phase):

$$\dot{m}_7 = \frac{\dot{m}_{LA,l}}{(1-Q)} \tag{12}$$

From the above equation, $\dot{m}_{LA,l}$ is the liquid air charge flow rate previously defined from *Table 10* for each of the systems, corresponding also to the flow rate in point 9 (*LAES Schematic system Charge Phase*) of the system. The term $\dot{m}_7$ is the mass flow of air before the separator, where this flow is a mix of liquid and vapour fraction of air, therefore, the vapour fraction corresponding in point 8 was found by the following equation:

$$\dot{m}_8 = \dot{m}_7 - \dot{m}_9 \tag{13}$$

Because in the Cold Box, a fraction of the air from the compressors is diverted to feed the Cryoturbines, with the objective to generate energy to reduce the specific consumption, the air mass flow from point 6 and 7 was the same, corresponding to the non-recirculation fraction from point 5. Therefore, using the set value of the recirculation fraction with the *equation 14*, the mass flow from the compressors was obtained.

$$\dot{m}_5 = \frac{\dot{m}_6}{(1-X_{RF})} \tag{14}$$

Now with the value of the mass flow at point, which is the same flow from point 1 to 4 because no flow losses are taken into account on the system, in another hand, the value used in the system recirculation was obtained with the *equation 15*.

$$\dot{m}_{10} = \dot{m}_5 - \dot{m}_6 \tag{15}$$

The value of mass flow in point 10 corresponds to all the flow that is transported to the cryoturbines, so this flow is the same for points 11 to 13. In order to know the flow from point 14 that goes through the Cold Box and which was the equivalent as the one that arrives at the beginning of the system at point 15, the corresponding flows from the cryoturbines and the air in the gas phase of the separator was added:

$$\dot{m}_{14} = \dot{m}_{13} - \dot{m}_8 \tag{16}$$

With the previous calculations, the mass flows used in the loading stage were obtained for each of the LAES plant sizes, detailed all this values in *Table 13*. Thanks to these values, the corresponding for the flow of energy used and generated in the load stage were found with the values for pressures and temperature.

Table 13. Mass Flow in Load Stage for each LAES system.

Point	LAES 1	LAES 2
1	166.553	333.105
2	166.553	333.105
3	166.553	333.105
4	166.553	333.105
5	166.553	333.105
6	103.263	206.525
7	103.263	206.525
8	140.024	280.048
9	892.602	17.852
10	6.329	12.658
11	6.329	12.658
12	6.329	12.658
13	6.329	12.658
14	772.924	154.585
15	772.924	154.585

2.2.2. Mass flow in discharge stage

For the discharge flow, it turns out to be equal at all points of this stage to the flow obtained from *Table 8*, because drops in the air mass flow ere not taken into account, therefore, *Table 14* corresponds to the flows for the discharge stage for each point of system.

Table 14. Mass Flow in Load Stage for each LAES system.

Point	LAES 1	LAES 2
16-26	35.7041	71.4082

2.3. Simulation parameters in DWSIM

With the initial parameters defined as turbine inlet temperature TIT, power output, system mass flow among others, *Tables 15* and *16* are constructed with the values of system pressure and temperatures, where these were alter completed with the use of the DWSIM. For the pressure drops, it was taken as a basis that 1% of the pressure was lost at each point of the system, taking the same losses form the reference [33], thus applying *equation 17* which represents the calculation procedure performed.

$$P_i = P_{i-1} * (1 - 0.01) \quad (17)$$

From the above, the *i* mean the point in systems where was obtained the pressure. In the system modelling, the pressures in points 7 to 9 and 13 to 15 correspond to the loading pressure of *Table 15*, used for the mapping modelling, due the previous points named was directly connected to point 9, being this same point to the one that represents the loading of the storage unit of the LAES tank. Of the initial parameters obtained from the basis reference for modelling, the underlining means that there were established according to the modelling data in *Table 15*, the bolded data means that these were established according to the simulator tool, and the other values mean that these were taken from the reference [33]. With the above, the results of *Table 16* were obtained for the load phase.

Table 15. Parameters selected for the performance maps of LAES plant in [32].

Parameter	Unit	SLAES
Charge Pressure (P_{ch})	Bar	50
Discharge Pressure (P_d)	Bar	75
Storage Pressure (P_s)	Bar	1.5
Utilization factor of HGCS (eta_{HGCS})	%	0,9
Utilization factor of HGWS (eta_{HWCS})	%	0,9

Table 16. Values used of the dimensioning of LAES plant Load Cycle [Adapted]. Source [33]].

Point	Pressure (bar)	Temperature (K)	Quality (-)
1	1.09	288.15	1.000
2	6.77	**517,75**	1.000
3	6.70	298,80	1.000
4	50.00	**542,82**	1.000
5	49.50	299.80	1.000
6	49.01	96.50	1.000
7	1.50	**82.31**	0.1356
8	1.50	**82.31**	1.000
9	1.50	**82.31**	0.000
10	49.01	**175.00**	1.000
11	**5.00**	**96.15**	1.000
12	**4.95**	**110.00**	1.000
13	1.50	**82.46**	1.000
14	1.50	**82.43**	1.000
15	1.50	**278.70**	1.000

During the calculation of the compression train between points 2 and 4, *equation 18* was used to find the pressure in each of the compression stages, using as final pressure to obtain 50 bar defined in the modelling maps and as initial pressure 1.09 bar.

$$R_C = \sqrt[n]{\frac{P_f}{P_i}} \tag{18}$$

P_f refers to the 50 bar from point 4, P_i the pressure before the compressor and *n* the number of stages. For discharge stage, the pressure after the air storage tank was taken as the same discharge pressure, therefore the temperature was the same at this point in the system. As in the loading procedure, the values in *Table 17* in bold were found by the DWSIM tool, those underlined with the use of *Table 15* and the others as the air quality, from the basis reference.

Table 17. Values used of the dimensioning of LAES plant Download Cycle [Adapted]. Source [34].

Point	Pressure (bar)	Temperature (K)	Quality (-)
16	1.50	82.31	0.000
17	75.00	**86.15**	1.000
18	74.25	**340.4**	1.000
19	73.51	426.33	1.000
20	**33.58**	**347.66**	1.000
21	**33.37**	430.00	1.000
22	**15.17**	**352.12**	1.000
23	**15.12**	435.00	1.000
24	**6.99**	**357.65**	1.000
25	**6.94**	440.00	1.000
26	**3.27**	**363.00**	1.000

In the point 19 of the discharge phase, to obtain the values of temperature and pressure, only the inlet temperature of turbine was taken, therefore, to complete the information with the other turbines, corresponding to point 21, 23 and 25, an increase in the temperature of its inlets was assumed, which was possible because the heat contribution was made by the HGWS, which can modify its mass flow to modify this contribution. The increase described, was approximately 5 K more between in the point and the next turbine in the process.

The temperatures and pressures described in the previous tables was not optimal for the operation of the system with a RT of 48 %, because these values were adapted to design a LAES plant with the map model of the reference [32] from zero, where additionally there is no consensus in the scientific community on the optimal operating values of a plant integration to any heat supply system. Additionally, in most cases, researchers have made use of advanced tool for each specific design LAES plant as Apsen HYSYS , being this tool licensed and advanced for its management for the develop in this project and not being able to use it in the same. However, with the information found in different literatures and with the used of DWSIM tool, the basic operating parameters described above was completed and his procedures will be explained in the next subsections.

2.4. Power block elements

With the obtained parameters of temperature, pressure, and mass flow in each element, in the DWSIM software it was possible to fin the power in the rest of units like the compressors, cryoturbines and cryopumps. The turbines were a known element because in the discharge phase, the output power was defined for each LAES plant, performing the respective calculations to convert the electrical power output from specific consumption formula of each plant, into the thermodynamic work of each turbine, the values of temperature and pressure of *Table 17* of the previous subsection were obtained. However, in this subsection Will detail the calculation made to obtain the turbine power to perform the simulation in the software.

2.4.1. Turbine

The mechanical and isentropic efficiency was established in 90% and 80 % respectively, where the mechanical efficiency was refers to the relation between the electrical power generated and the mechanical power produced, as detailed in *equation 19*. For the above, it was related that the output power of each LAES system corresponds to the electrical power it would contribute to the grid, therefore, with the use of this equation, the mechanical power of the turbine system was obtained, where is detailed in the figure of *LAES Schematic system Discharge Phase*, each system was be made up of 4 turbines.

$$\eta_{mec,t} = \frac{P_{e,t}}{P_{mec,t}} \tag{19}$$

The detailed results of the mechanical power in each turbine are summarized in *Table 18*. The real power obtained from the turbine was defined as the same mechanical power, because the objective was to simplify the modelling of the discharge system, detailed in *equation 20* the isentropic efficiency. Thus, it was possible to obtain the isentropic power, however, by entering the mechanical power and isentropic efficiency data in DWSIM program, the power with isentropic work and the best values of temperature and pressure were obtained, which will achieve the established power for each LAES plant.

$$\eta_{iso,t} = \frac{P_{mec,t}}{P_{iso,t}} \tag{20}$$

Table 18. Mechanical and Electrical Power in Turbines for each LAES system.

	LAES 1		LAES 2	
Element	**P_{mec} [kW]**	**P_{ele} [kW]**	**P_{mec} [kW]**	**P_{ele} [kW]**
Turbine 1	2777	2500	5555	5000
Turbine 2	2777	2500	5555	5000
Turbine 3	2777	2500	5555	5000
Turbine 4	2777	2500	5555	5000

2.4.2. Compressor

For the compression stages, the inlet and outlet pressures for each stage had defined from the previous sections. With this in the software it was possible to obtain the other

missing variables such as the outlet temperature in order to find the output power of each compressor. Since it was assumed, as in the case of the turbines, that the real power corresponds to the mechanical power, and this found in the software, *equations 21* and *22* were applied to find the electrical power that would be consumed by the compression train.

$$\eta_{iso,c} = \frac{P_{iso,c}}{P_{mec,c}} \tag{21}$$

$$\eta_{mec,c} = \frac{P_{mec,c}}{P_{ele,c}} \tag{22}$$

The results of the power founded in the software is detailed in the *Table 19*, where show the mechanical o real power done by the compressor, and the electrical power consumed by the same. With the program, isentropic and mechanical power were found, taking efficiency of 89%, therefore, the *equation 21* was developed by the same program. On the other hand, to find the electrical power that would be consumed by the compressors, *equation 22* was applied to the result of the mechanical power obtained by the program.

Table 19. Mechanical and Electrical Power in Compressors for each LAES system.

	LAES 1		LAES 2	
Element	**P_{mec} [kW]**	**P_{ele} [kW]**	**P_{mec} [kW]**	**P_{ele} [kW]**
Compressor 1	3685.53	4095.03	7370.58	8189.53
Compressor 2	4371.31	4857.01	8742.48	9713.87

2.4.3. Cryoturbine

To obtain the work of each cryoturbine, the project did not specify in depth the definition of the optimal parameters, but the most appropriate results were sought according to literature. Due to the above, the pressures and temperatures were adjusted from the DWSIM software to obtain a reduction in the specific consumption of the cryoturbine.

The real power supplied by each cryoturbine were founded, summarized in *Table 20*, also the electrical power that would supply and contribute to the system was found. This element in the design process was found in the literature that its design for the plants is very ambiguous, where there can be configuration of different amount of cryoturbines, where in some cases it is possible to do without it [41]. However, in this work it was included to know the actual contribution to the loading process.

Table 20. Mechanical and Electrical Power in Cryoturbines for each LAES system.

	LAES 1		LAES 2	
Element	**P_{mec} [kW]**	**P_{ele} [kW]**	**P_{mec} [kW]**	**P_{ele} [kW]**
Cryoturbine 1	327.86	295.07	655.72	590.15
Cryoturbine 2	149.87	134.88	299.74	269.76

As detailed in *Table 20*, the power input is minimal compared with the power consumed from compression train, but sufficient for use in possible auxiliary systems. The explanation for the fact that systems include it was due to the fact that, it was possible to obtain more liquid air and, in turn, obtain an electrical contribution to the system [42].

2.4.4. Cryopump

Fort the work done by the cryopumps; the program helped to find the temperature obtained when the liquid air was compressed to the 75 bar discharge established in the design parameters. The results obtained of real o mechanical power are detailed in *Table 21*, where the electrical power consumed for each LAES plant reaches a maximum of 4,22% of the electrical power generated by the turbines, for this reason this power was not taken into account for the calculation of the discharge flow.

Table 21. Mechanical and Electrical Power in Cryopump for each LAES system.

	LAES 1		LAES 2	
Element	**P_{mec} [kW]**	**P_{ele} [kW]**	**P_{mec} [kW]**	**P_{ele} [kW]**
Cryopump	380.61	422.61	760.624	845.13

2.5. HGCS and HGWS tank

Detailed the main elements of power, we proceeded to fin the values of heat and cold provided by the High Grade Cold Storage (HGCS) to the system, this through the Cold Box, and the High Grade Warm Storage (HGWS). This was done with the process simulation software, where for the HGCS, the values of heat provided and given in the Cold Box were taken and using the energy transfer formulas of the reference [32]. For the HGWS, the heat contributed on the compression was obtained and compared with the heat received in the discharge stage.

For the corresponding calculations for the dimensioning of these systems, the fluids referenced for HGCS and HGWS from the base literature were used, the former being air of the same composition as that used in the system; for the HGWS it was thermal oil, with a density ρ=750 kg/m3 and a specific heat c=2200 J/kg K [32], for HGCS was used air. The temperatures and pressures established to perform the heat exchange of these systems were also based on the base reference, summarized in *Table 22*. From the processes developed in this section, it is clarified that it was performed in a basic way, because the objective of the process developed in this section was to find the approximate flow and tank sizes, to comply with the energy balance in the transfer with the contributions of the HGCS and HGWS.

Table 22. Temperatures and Pressures used in HGCS and HGWS. Source [34].

Point	Pressure (bar)	Temperature (K)
1C	1.50	278.2
2C	1.49	92.7
3C	1.50	93.0
4C	1.49	278.7
1H	1.10	288.2
2H	1.09	661.8
3H	1.09	82.31
4H	1.09	82.31

The points corresponding to the HGCS were 1C, 2C, 3C and 4C, the first two obtaining the cold from the discharge stage and the last two contributing cold to the Cold Box. The points from 1H to 4H correspond to the HGWS, where from point 1H, the flow is divided between 2H and 3H, which obtain the heat form the compressors, then these flows are joined in 4H. The above is detailed in *Figure 7* and *8* of the stages of charge and discharge from document section 4.

2.5.1. HGCS system mass flow

To calculate the mass flow of the system, first we obtained the values of heat provided and given in the Cold Box except for the hear provided by the same HGCS, the above with the use of simulator process. *Table 23* shows the heat supplied in point 11 to 12, 14 to 15, and heat removed in points 5 to 10 and 5 to 6 in the Cold Box.

Table 23. HGCS Heat contributed and received.

Points	Heat Transfer	LAES 1 [kW]	LAES 2 [kW]
11-12	Heat Added	118.82	237.64
14-15	Heat Added	1734.71	3469.37
5-10	Heat Removed	1044.37	2088.71
5-6	Heat Removed	4223.54	8446.96

With the values obtained from *Table 23*, an energy balance represented in *equation 23* and obtained for the ideal operation of the Cold Box was used, being the cold contributed those corresponding to the sub-index *c* and the cold received or added with the *h*. Since the HGCS system is a cold contribution system, the corresponding equation to find the necessary heat is expressed in *equation 24*.

$$\phi_h = \phi_c \tag{23}$$

$$\phi_{c,HGCS} = (\phi_{h,5-10} + \phi_{h,5-6}) - (\phi_{c,11-12} + \phi_{c,14-15}) \tag{24}$$

The contribution of the HGCS is essential for the airflow of points 5-6, being this the main flow which mostly the Cold Box obtains a fraction of air vapor defined above (*Table 12)*. From the previous process, the values of cold contribution that would be made in each LAES system are obtained in *Table 24*.

Table 24. Heat contribution in HGCS.

Element	LAES 1 [kW]	LAES 2 [kW]
HGCS	3414.38	6828.66

With the latent heat values of HGCS from *Table* 24, the temperatures from *Table 22* at point 4C and 3C and the air density at point 4C calculated by CoolProp tool (ρ=1006.75 kg/m^3); the *equation 25* was applied, where the unknown of the mass flow is cleared and calculated with the previous data. The points 4C and 3C are chosen for the calculation because the system load phase was developed first and the critical phase in the cycle is the cold share in the Cold Box.

$$\phi_{c,HGCS} = \dot{m}_{4C} * Cp_{air,4C} * (T_{4C} - T_{3C}) \tag{25}$$

The mass flow obtained in the loading phase for the HGCS is detailed in *Table 25*, where it was possible to obtain the mass flow in the unloading stage, because the previously calculated stored head discharge into the Cold Box is theoretically the same as the heat obtained in the unloading phase, of the system after the expansion of the air in the cryopump. Even so, in this process it was considered that of that available energy, only 90% could be used due to the parameters defined in the modelling.

Table 25. Mass flow in download stage of HGCS.

Mass Flow	LAES 1 [kg/s]	LAES 2 [kg/s]
3C,4C	18.26	36.52
1C, 2C	90.23	185.17

2.5.2. HGCS size tank

In literature base proposes that a packed bed storage tank made up of cylinders is the best option for storing air. From the above, *equation 26* was derived from the reference for [38] for the calculation of the size in volume of the tank that would store the air to be cooled in the Cold Box.

$$V_{HGCS} = \frac{\dot{m}_{1C}(h_{1C} - h_{2C})t_l}{\rho_s c_s(1-\varepsilon)(T_{4C} - T_{3C})} \quad (26)$$

From the above, the calculation of the enthalpies at h_{1C} y h_{2C} was develop with the CoolProp library in Python. The density of the material in the cylinders ρ_S, the specific heat capacity c_S and the void fraction ε values was taken from the reference [38], being 2560 kg/m^3, 541 J/KgK y 0,38 the respective values. From the above data, the results of the equation 26 is detailed in the *Table 26*.

Table 26. HGCS size in volume.

Parameter	Unit	LAES 1	LAES 2
Storage	m^3	789.32	1579.64

Once the process to know the capacity in energy of the HGCS was done, the values of the *Table 24* were multiplied with the load charge time of the system of 8 hours, where in the *Table* 27 is detailed the total energy store for each tank in each system.

Table 27. Theoretical energy storage.

Element	LAES 1 [MWh]	LAES 2 [MWh]
HGCS	27.31	54.63

2.5.3. HGWS system mass flow

The heat input for the HGWS system is provided by the compressor to be used in the discharge stage of the turbines. With the help of the DWSIM software, the heat values obtained by the compressors in the charge stage of the LAES system by means of the Intercoolers were found; on the other hand, the heat that the turbines would need to operate according to the chosen parameters and that would by provided by the HGWS by means of the Superheater was found. From the above it was found that, of the input received from the compressors, less than 90% of the stores heat is used in the discharge

process in the turbines, due the above, the sizing and mass flow was carried out with the input obtained from the compressors.

Table 28. HGWS share of heat in charge and discharge stages.

Element	LAES 1 [kW]	LAES 2 [kW]
Intercooler 1	3888.31	7776.51
Intercooler 2	5045.45	10090.74
Superheater 1	3689.09	7377.34
Superheater 2	3421.46	6842.61
Superheater 3	3375.11	6750.16
Superheater 4	3324.96	6649.88

With *Table 28* above that detail the heat input to the HGWS by the intercooler and the input to the system with the superheaters, the energy input from the compressor and the energy expenditure for preheating the air in the turbines were obtained by multiplying by the loading and unloading times of the system. The energy obtained from the compressors is three times the energy needed to preheat the air, as shown in *Table 29*, therefore only highest value of energy input obtained from the intercooler was taken, taking into account that there is a heat loss which it was not possible to identify.

Table 29. HGWS share of energy in charge and discharge stage.

Elements	LAES 1 [MWh]	LAES 2 [MWh]
Intercooler	71.47	142.94
Superheater	27.62	55.24

With the use of the heat flow formulas, *equation 27* is obtained to be used in the HGCS, where with this formula the approximate flow was found for each point to comply with these formulas, where the heat supplied to the HGWS is the total heat made by the intercooler, the specific heat Cp_{4H} was obtained from the reference [36], which corresponds to thermal oil.

$$\phi_{HGWS} = \phi_{I1} + \phi_{I2} = \dot{m}_{4H} * Cp_{4H} * (T_{4H} - T_{1H}) \quad (27)$$

From the above equation, the results of the detailed mass flow rates in *Table 30* were obtained, for which it is clarified that this the flow rate used for the storage tank sizing calculation.

Table 30. Mass flow in HGWS system.

Element	LAES 1 [kg/s]	LAES 2 [kg/s]
1H, 4H	10,21	20,42

2.5.4. HGWS size tank

With the values obtained from the mass flow in the loading stage of the system, the size of the storage tank is obtained with *equation 28*, obtaining in weight what the HGWS

tank should support of thermal oil. With this result, it was possible to get the size in terms of volume by using the density of the thermal oil, above with the help of *equation 29*.

$$m_{HGWS,tank} = t_l * \dot{m}_{4H} \tag{28}$$

$$V = \frac{m_{HGWS,Tank}}{\rho_{oil}} \tag{29}$$

The sizes of the HGWS system for each LAES plant are detailed in *Table 31*, where this value was used for the economic calculation of the system. It is clarified that although the heat input used does not reach the 90% established in the design parameters, it is sized in the same way with the maximum input made in the compression stage.

Table 31. HGWS size in volume.

Parameter	Unit	LAES 1	LAES 2
Storage	m^3	392.14	784.28